

Demyelination and Trans Synaptic Degenerative changes in the Visual Pathway in Glaucoma

Samran Sheriff

BMedSci (Immu)., M. Orth.

A Thesis in Publication Submitted in Partial Fulfilment of the Requirement of the Degree
of Master of Research in Clinical Medicine (MResClin)



Department of Clinical Medicine
Faculty of Medicine and Health Science
Macquarie University
NSW Australia

Presented on the 21st of April 2019

Table of Contents

Table of Contents.....	i
List of Tables.....	iii
List of Figures.....	iii
Statement of Original Authorship.....	iv
Acknowledgements	v
List of Publications	vii
List of Contributors/Contributions	vii
List of Abbreviations.....	ix
Abstract.....	x
1. Introduction	1
1.1. The Brain and Neurodegeneration.....	1
1.1.1. White Matter Tracts in the Brain.....	2
1.1.2. The Spread of Neurodegeneration along White Matter tracts – Trans Synaptic Degeneration (TSD)	3
1.2. The Visual System.....	4
1.2.1. Visual Projections - From the Eye to the Brain.....	6
1.2.2. The Visual Pathway Model	7
1.2.3. Glaucoma and Secondary Neurodegeneration in the Brain	8
1.2.4. Risk factors and Clinical Management	10
1.2.5. Glaucoma and Neurodegeneration along the Optic Nerve.....	11
1.3. Monitoring Neurodegenerative changes in the Visual Pathway.....	12
1.3.1. Optical Coherence Tomography (OCT).....	12
1.3.2. Retinal Nerve Fibre Layer (RNFL) and Glaucoma.....	13
1.3.3. Diffusion Tensor Imaging and Tractography	16
1.3.4. Visually Evoked Potential (VEP).....	18
1.3.5. Humphrey Visual Field (HVF).....	18
1.4. Hypothesis and Research Plan	21
1.5. References	22
2. Association between Studies.....	27
3. Quantification of MRI parameters against demyelination in the white matter: A systematic analysis of post mortem quantitative imaging and histopathological studies	28
3.1. Abstract	28
3.2. Introduction.....	29
3.3. Methods	30

3.3.1.	Overview of Review Method	30
3.3.2.	Data sources and Chosen Search Strategy.....	30
3.3.3.	Study Selection.....	31
3.3.4.	Data Extraction and Quality Assessment	31
3.3.5.	Statistical Methods	32
3.4.	Results.....	32
3.4.1.	Identification and Selection of Studies	32
3.4.2.	Study Characteristics and Geographic Distribution	33
3.4.3.	Correlation between MRI parameters and variables against either (ML/AL).....	33
	Identification.....	39
	Screening.....	39
	Eligibility	39
	Included	39
3.5.	Discussion.....	40
3.6.	Supporting Info	44
3.7.	Appendices.....	44
3.8.	References	48
4.	Normal adjusted RNFL analysis against MRI diffusion parameters within a glaucoma cohort.....	51
4.1.	Abstract.....	51
4.2.	Introduction	52
4.3.	Methods.....	53
4.3.1.	Data Collection.....	53
4.3.2.	Spectral Domain Optical Coherence Tomography Imaging.....	54
4.3.3.	MRI Data Acquisition.....	55
4.3.4.	Statistical Methods	55
4.4.	Results.....	56
4.4.1.	Patient Characteristics	56
4.4.2.	Normalised Ratio Calculation.....	57
4.4.3.	Mean MRI diffusion parameters	58
4.6.	Discussion.....	60
4.8.	References	62
5.	Future Directions.....	64
5.1.	Progression of Trans Synaptic changes in the Glaucoma Cohort	64
	Appendix.....	66

List of Tables

Table 1.1. Key MRI parameters measured during Diffusion Tensor Imaging of various neurological conditions.....	17
Table 1.2. Various Methods of MRI Myelin Quantification.	20
Table 3.1. Demographic Data of studies included in Analysis.	35
Table 3.2 Relationship between MRI parameters and ML/AL (R2).....	36
Table 4.1. Average calculated affected and unaffected MRI indices across twenty-four patients.	58
Table 4.2. Correlation between RNFL thickness and DTI variables from twenty-four patients.	58

List of Figures

Figure 1-1. Pathway of the Human Visual System.	5
Figure 1-2. Range of Cup to Disc ratio (CDR).	9
Figure 1-3. Optical Coherence Tomography (OCT) – Carl Zeiss OCT.	14
Figure 1-4. Optical Coherence Tomography (OCT) – Heidelberg OCT Spectralis. ..	15
Figure 1-5 Humphrey Visual Field Analysis - Glaucoma	19
Figure 2-1. Position of Individual articles (Paper 1 & Paper 2) within various thematic areas.....	27
Figure 3-1 Pooled weighted correlation coefficient depicting MRI parameters analysed across various studies against Myelin Loss (ML).	37
Figure 3-2 Pooled weighted correlation coefficient depicting MRI parameters analysed across various studies against Axonal Loss (AL).	38
Figure 3-3 (PRISMA) Flow Diagram of Study Selection Protocol	39
Figure 4-1 Heidelberg Spectralis Axonal single exam report OU printout of a RNFL	56
Figure 4-2 Mean +/- SEM for RNFL thickness in the study population	57
Figure 4-3 Relationship between Retinal nerve fibre layer (RNFL) thickness (um) and each of the four MRI diffusion parameters between the affected and unaffected optic radiations (OR) in POAG.....	59

Statement of Original Authorship

The thesis titled 'Demyelination and Trans Synaptic degenerative changes in the visual pathway in Glaucoma' and the work associated with the creation of this thesis has to the best of my ability not previously been submitted for a degree or diploma at any other higher education institute. The work contained in this thesis is all original research conducted by myself. Any assistance received during the creation has been properly acknowledged in appropriate form and context.

The research presented in this thesis has been approved by the University of Sydney and Macquarie University. Ethics Approval No. 2013/106.

Signed:

Date: 21/04//2019

Acknowledgements

In the last 10 months I have learnt and grown immensely not only as a clinician but as a person than I ever thought imaginable. The following people have been invaluable in the process and for that I would like to thank them personally.

First and foremost, I must thank and acknowledge my associate supervisor Dr Yuyi You.

Dr You, thank you for the opportunity, the privilege and the guidance you provided me during this MRES period. Under your supervision I learnt how to practice good and honest science, beyond this I was exposed to the attributes that make an excellent and well-respected researcher, learning the true meaning of professionalism within the field. It has been a pleasure working under your supervision and I thank you once again for the countless hours that you spent editing my work, suggesting improvements and being there for moral and emotional support. I hope that our paths cross again someday.

Professor Stuart Graham. Thank you for the wonderful privilege to be accepted as a member of your research team. You were there for any clarification that I needed, and it was very comforting knowing that such an experienced ophthalmologist was my supervisor. You were able to instil in me the traits of a good team member, knowing when to work independently and when to seek guidance, skills that I will carry well into my career.

Dr Vivek Gupta. Thank you immensely for helping me out within the office on a day to day basis throughout the entire candidature. Through collaboration with yourself I was able to appreciate the value of efficient planning and effective trouble shooting.

Secondly, I would like to thank all the members of the Graham research group for your loving and caring nature and in particular those that contributed to my project along the year.

Ting Shen. Thank you for your help with the initial set up of project and ethics applications. I hope your PhD goes well.

Linda Garthwaithe. Thank you for all your countless help with fixing up my grammar throughout the year.

To my fellow MRES students: Angela Godinez and Danit Saks. It's been such a fun ride and I could not have asked for two better people to share the journey with. Our bonding over the highs and lows of research has really brought us together on a deeper level and I loved every minute of it. The spontaneous lunches and countless trips to Macquarie centre will be missed a lot.

To Dr. Jen Rowland, I can't thank you enough for all your help and assistance throughout the MRES program. You have been an excellent director and I wish you all the best in the future. Thank you immensely for helping me with my thesis preparation, this whole thing would not be possible without you.

A big thank you goes out to all the participants that took their time out of their schedules to be part of a great cause. This project and countless others would not have been possible without people like you and it was lovely meeting each and every one of you. To everyone at the Brain and Mind Research Centre, thank you for all your support and help with the clinical phase of this study. Prof Klistorner your on the spot advice and lectures still resonate with me and I am truly grateful for your guidance.

Finally, thank you to my family. You have been there to support me all the way through this and I cannot express how grateful I am. Nashwa, my little sister I love you to bits, thank you for actively making me pursue my dreams and goals. I hope I have made you, Mom and Dad proud.

I Dedicate this Thesis to my Parents.

List of Publications

1. **SHERIFF, S.**, KLITORNER, A., GUPTA, VK., GRAHAM, SL., YOU, Y. 2018. Quantification of MRI parameters against demyelination and axonal loss in the white matter: A systematic analysis of post mortem quantitative imaging and histopathological studies. (*Intended Journal for Review/Publication - Neurology*)
2. **SHERIFF, S.**, KLITORNER, A., GUPTA, VK., GRAHAM, SL., YOU, Y. 2019. Retinal Nerve Fibre Layer Analysis against MRI diffusion parameters (*Manuscript in Preparation*). (*Intended Journal for Review/Publication – Investigative Ophthalmology and Visual Science IOVS*)

List of Contributors/Contributions

Principal Supervisor:

Dr Vivek Gupta. Faculty of Medicine and Health Sciences, Department of Clinical Medicine, Macquarie University.

Associate Supervisors:

Prof. Stuart Graham. Faculty of Medicine and Health Sciences, Department of Clinical Medicine, Macquarie University.

Dr Yuyi You. Department of Ophthalmology, Save Sight Institute, The University of Sydney.

Division of Labour in Co-Authored Articles

SS- Samran Sheriff; YY – Yuyi You; VK- Vivek Gupta; SLG – Stuart Graham; AK- Alexander Klistorner

	Paper 1	Paper 2
Data Curation	SS, YY	SS, YY
Formal Analysis	SS, AK, YY	SS, YY
Investigation	SS, AK, YY	SS, SLG, YY
Methodology	SS, AK, YY	SS, SLG, YY
Writing- Original Draft	SS	SS
Writing – Review and Edits	SS, AK, YY	SS, YY
Supervision	VG, SLG	YY, SLG

List of Abbreviations

ACG	Angle Closure Glaucoma
AD	Alzheimer's Disease
AD	Axial Diffusivity
ADC	Apparent Diffusion Coefficient
ARMD	Age Related Macular Degeneration
BCVA	Best Corrected Visual Acuity
CNS	Central Nervous System
CST	Cortical Spinal tract
DTMRI	Diffusion Tensor Magnetic Resonance Imaging
DTI	Diffusion Tensor Imaging
FA	Fractional Anisotropy
LGN	Lateral Geniculate Nucleus
MD	Mean Diffusivity
ML	Medial Lemniscus
MS	Multiple Sclerosis
MTR	Magnetization Transfer Ratio
MWF	Myelin Water Fraction
MRI	Magnetic Resonance Imaging
NAWM	Normal Appearing White Matter
OCT	Optical Coherence Tomography
OR	Optic Radiations
PNS	Peripheral Nervous System
POAG	Primary Open Angle Glaucoma
RD	Radial Diffusivity
RGC	Retinal Ganglion Cell
RNFL	Retinal Nerve Fibre Layer
TSD	Trans Synaptic Degeneration
T1	T1 Relaxation Time
T2	T2 Relaxation Time
V1	Visual Area 1
V2	Visual Area 2
V3	Visual Area 3
VEP	Visual Evoked Potential
VP	Visual Pathway
WHO	World Health Organisation

Abstract

Neurodegenerative disorders are characterised by irreversible neuronal loss, to which the exact mechanism remains unknown. One feature of neurodegenerative disease; Trans Synaptic degeneration (TSD) plays a key role in many CNS diseases such as Alzheimer's disease, Multiple Sclerosis and Optic Neuritis. Diffusion Tensor Magnetic Resonance Imaging (DTMRI) allows us to measure and visualise the orientation and anisotropy of MRI parameters in vivo.

These measurable parameters can be used to characterise tissue integrity in the brain and white matter and thus show microstructural changes that are occurring throughout the disease process.

This study looks to investigate which MRI parameter/s are measuring demyelination and whether demyelination is the initial pathological change that is occurring in glaucoma. These aims will be addressed in two phases, firstly a meta-analysis will be conducted in order to identify which MRI parameter/s is directly measuring demyelination and axonal loss. Followed by a comprehensive analysis comparing adjusted retinal nerve fibre layer (RNFL) thickness and MRI parameter values in the visual pathway in glaucoma patients. The clinical study will therefore allow us to identify which MRI parameter/s recognized from phase 1 are directly responsible for micro structural changes that are seen.

Keywords – (Post Mortem AND Post-Mortem), (MRI), (Demyelination), (Axonal Loss), (Histology), (Glaucoma), (Optical Coherence Tomography), (Retinal Nerve Fibre Layer)

1. Introduction

1.1. The Brain and Neurodegeneration

Neurodegeneration is the disease process that results from the progressive loss of structure and function of neurons located particularly in the central nervous system (CNS). The diseases in which neurodegeneration is most prevalent are those that most commonly affect the elderly or occur in societies with a relatively longer life expectancy. Alzheimer's Disease (AD), Parkinson's Disease and Multiple Sclerosis (MS) are some of the most common and well known neurodegenerative diseases in the 21st century [1] , and are a major cause of morbidity and added financial burden on the health and social welfare systems and as a result have gained increased recognition by the World Health Organisation (WHO).

The progression of neurodegenerative diseases is characterised by the gradual onset of neurological symptoms; (i.e. memory loss, loss of motor skills, spatial dysfunction, language difficulties) as is characteristic in the aforementioned diseases.

One of the human brain's primary functions is visual processing. The occipital lobe located on the posterior surface, is the main cortical region involved in visual perception. Of the total mass of neuronal brain cells, over 30% of the human cortex is devoted to visual processing, as compared to 8% for proprioception and 3% for auditory processing [2, 3]. There is increasing literature evidence suggesting that the human eye is an extension of the central nervous system with the retina in particular sharing many physiological, cellular and biochemical similarities with the brain [4, 5].

Neurodegenerative conditions that impact the CNS functioning usually also have clinical ocular manifestations, due to the eye's distinct anatomical location, being located anteriorly and superficially. Pathological processes are more clinically measurable in the eye as compared to other parts of the CNS [4]. The retina and optic nerve are two structures located in the visual system of humans that can be easily accessed and imaged both through in vivo and ex vivo methods and are thus widely used as models to study neurodegenerative disorders; such as Alzheimer's Disease [13, 44] and Multiple Sclerosis [56].

1.1.1. White Matter Tracts in the Brain

White matter (composed of glial cells and myelinated axons) makes up one of the two key components of the central nervous system. The other main component being grey matter (neurons). White matter in the CNS is primarily responsible for conduction impulses that increase the electrical activity of nerve impulses thereby increasing their speed of transmission [6], with myelin acting as an insulator in this process. White matter makes up 2% of the total long range fibres within the human brain with the corpus callosum being the largest white matter structure [6].

The recent advancement in neuroimaging techniques such as Magnetic Resonance Imaging (MRI) and Diffusion Tensor Imaging (DTI) has allowed and advanced the field of neurology allowing virtually any white matter structure in the CNS to be imaged.

Within the brain, white matter is classified into three categories; Projection Tracts, Association Tracts and Commissural Tracts [7].

1.1.1.1. *Projection Tracts*

Projection tracts are the names given to the long spanning fibre projections of the brain that connect the cortex with other CNS nuclei, i.e. connect higher and lower brain and spinal cord centres. These are classified as either afferent (sensory) tracts projecting to the CNS or efferent (motor) projecting to effector organs. Examples of common projection tracts located within the CNS and PNS include; The Corticospinal Tract (CST), Medial Lemniscus (ML) and **Optic Radiations (OR)**. The latter of which will be discussed in more detail [7].

1.1.1.2. *Association Tracts*

The brain can be divided into two hemispheric lobes. Association tracts are tracts that connect different areas within the same lobe. Diffusion Tensor Imaging (DTI) can identify structures such as; arcuate fasciculus, superior and inferior occipito-frontal fasciculus, the cingulum, uncinate and in particular the inferior longitudinal bundle that connects the anterior temporal lobe and the extra striate cortex of the occipital lobe [7].

1.1.1.3. *Commissural Tracts*

These are the tracts that connect the same cortical area in opposite hemispheres. The corpus callosum is the main commissural tract of the human brain together with the anterior and posterior commissure [5, 7]. It is through commissural tracts that the corresponding left and right cerebral hemispheres are able to communicate with each other.

1.1.2. The Spread of Neurodegeneration along White Matter tracts – Trans Synaptic Degeneration (TSD)

Trans Synaptic degeneration is defined as the spread of neurodegeneration along white matter tracts, from the first order presynaptic neuron to the second order post synaptic neuron. Initially described by Van Buren (1963) [66] following occipital lobectomy in a macaque, the process of TSD can be observed to be bidirectional (both anterograde & retrograde).

Degeneration of neurons following isolated injury is a known phenomenon resulting in cell body and axonal injury. The loss of an isolated population of neurons can lead to secondary degeneration of neurons to whom they provide significant afferent and efferent connections [9]. This spread of neurodegeneration has been reported in motor and cerebellar pathways in humans, however its role in the visual system has not been well defined. Recent advancements in ocular imaging such as Optical Coherence Tomography (OCT) and diffusion MRI have provided increasing evidence for retrograde trans synaptic degeneration (RTSD) in the human adult visual system.

There are various mechanisms by which TSD occurs along White Matter (WM) tracts. The type of TSD seen mainly in humans is bidirectional, (anterograde and retrograde) resulting from lesions in the brain or white matter pathways [10] (See Figure 1-1). Lesions to specific white matter tracts cause pathological changes within axonal bodies and lead to whole system degeneration. Brain lesions along white matter tracts result in structural and transient interruption of sensory input via damage of neuronal fibres, resulting in loss of excitatory input to other cortical areas, down regulating them to excitation stimuli, the typical pathophysiology that is common in cases of MS and AD.

TSD following lobectomy was first described in 1963, where TSD occurred after sudden loss of input stimuli from the olfactory bulb (Van Buren, 1963) [11, 66]. Van Buren was able to demonstrate that following left hemispheric removal in monkeys resulted in retrograde TSD of RGC's , which has since been demonstrated in vivo with the advancement of OCT in humans [12].

White matter tracts in humans are composed of dendritic and axonal components. RTSD affects both these structures at the cellular level with evidence of shrinkage and apoptosis in the main dendritic shaft following TSD. The loss of excitatory input results in mitochondrial swelling and dense packing of microtubules [13].

TSD in the visual system has become an area of interest in the field of neurology due to its involvement with visual impairment, and that the process of TSD is thought to underline atrophy in particular disease states. The visual system in humans may represent a simple model for understanding the mechanisms behind TSD. Glaucoma is considered a neurodegenerative disease and is diagnosed based on optic nerve atrophy and visual field defects and accounts for one of the leading causes of worldwide blindness. TSD in glaucoma was first hypothesised by (Gupta and Yucel 2007) and through the recent development in MRI and OCT technology this hypothesis has been further explored in various studies [10, 14, 15].

1.2. The Visual System

Considered an extension of the CNS, the visual system in humans allows the processing of visual detail from visible light to build a representation of the surrounding environment [4, 5]. The cornea and lens are considered the main refractive media, with slight input from the aqueous and vitreous humour thereby, refracting visible light into a small image on the retina. Electrical transduction within the retina passes this information to the Optic nerve CNII, through the optic canal. At the optic chiasm the nerve decussates and the fibres branch and terminate in the primary visual cortex (V1).

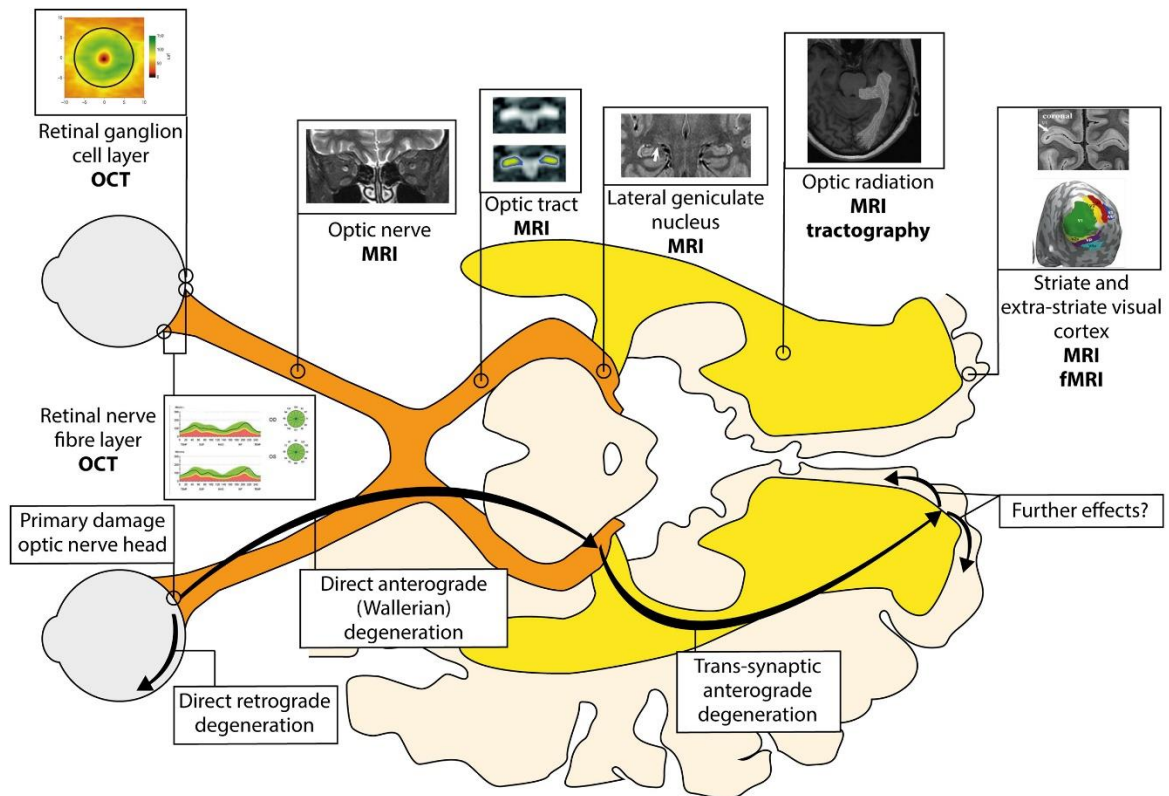


Figure 1-1. Pathway of the Human Visual System and various Neuroimaging Techniques. Black tract representing flow of visual input from retina to occipital cortex. Various methods of neurodegeneration highlighted along the visual pathway with corresponding neuroimaging techniques used for monitoring progressive changes.
(Images taken with permission from Lawlor et., al 2018) [8].

1.2.1. Visual Projections - From the Eye to the Brain

The visual pathway can be further subdivided into the anterior and posterior pathways. The anterior pathway comprises structures from the eye to the LGN (Lateral Geniculate Nucleus) (See Figure 1-1) and the posterior pathway; from the LGN to the Striate and extra- striate cortex [16, 17] (See Figure 1-1).

After light has been processed by the retina, electrochemical detail regarding the image is sent along the optic nerve. Ganglion cells located in the retina send different signals to the brain via this nerve, with 90% of the axons involved terminating at the LGN. The other 10% are sent to the superior colliculus located in the midbrain for assistance with controlling eye muscle movement (saccades) [16, 17].

1.1.1.4. *Optic nerve, Chiasm and Tracts*

RNFL (retinal nerve fibre layer) axons converge and exit the back of the eye as the optic nerve. Comprised of over 1.2 million RGC axons located in the RNFL, information from both nerves is combined and arranged accordingly into the patient's visual field. The corresponding right and left fields of view are sent to the left and right halves of the brain I.e. the right visual cortex is focused on the left field of view and vice versa. This strict topographic arrangement is maintained from the RGC to the LGN. Superior fibres run superiorly, and inferior fibres run inferiorly along the nerve, with the temporal and nasal fibres running on corresponding sides. Surrounding the nerve is myelin, making the optic nerve a white matter tract in the brain and vulnerable to neurodegenerative diseases such as MS and glaucoma [17]. The post chiasm portion of the visual pathway is the left and right optic tract and contains the ipsilateral temporal retinal RGC's and the Contralateral nasal RGC's, terminating at the LGN (See Chapter 4 for RNFL study).

1.1.1.5. *Lateral Geniculate Nucleus*

The LGN is the sensory relay point in the visual system. The LGN consists of six layers in humans. Layers 1,4,6 contain information from crossed fibres of the nasal retina (temporal visual field) and layers 2,3,5 contain information from the ipsilateral (uncrossed) fibres of the temporal retina (nasal visual field). Neurons from the LGN project via the optic radiations to the calcarine cortex of the occipital lobe [16].

1.1.1.6. *Optic Radiations and Visual Cortex*

The RGC neurons that reach the optic radiations are third order neurons of the visual system. The optic radiations are located on each side of the brain and before reaching the cortex take an anterior course through Meyers Loop. The topographic arrangement is still maintained at the level of the cortex i.e. temporal radiation fibres correspond to the contralateral superior visual field and parietal radiations represent the contralateral inferior field.

The human visual cortex area 17 is the largest system in the brain and is located posteriorly, above the cerebellum [16, 18]. The area that receives the information from the LGN via the optic radiations is termed the primary visual cortex (V1). Visual input from this system then flows hierarchically to V2, V3, V4 and V5 sequentially. These association areas process a range of stimuli such as orientation, edge support, corner detection and basic information regarding processing of colour and motion [19].

1.2.2. The Visual Pathway Model

Neurodegenerative diseases continue to evolve into the broader perspective with symptoms such as inflammation, axonal loss and myelin loss being used as markers of disease progression [20, 21]. Alternatively, there has emerged the need to document progression of the disease in a non-invasive way. The visual pathway model (VP) offers several advantages in studying neurodegenerative diseases [16].

The posterior aspect of the eye can be thought of as the front of the brain. The eye can be considered an extension of the CNS and due to its highly coherent topographic arrangement, the anterior visual pathway can mirror CNS effects of tissue specific injury in neurodegenerative disease [22]. The visual pathway model is a nervous system model and deficiencies within this system can be captured and reproduced. BCVA (best corrected visual acuity), automated perimetry, colour vision testing and in particular optical coherence tomography (OCT) and visual evoked potentials (VEP) can explore and show the structural and functional integrity of the VP model. Based on this we can elucidate the

contributions of inflammation, axonal loss and neuronal damage in the VP model of glaucoma [6].

The VP model has also shown potential in identifying tissue specific and whole system specific factors that play a role in injury and tissue repair in neurodegenerative diseases [23].

1.2.3. Glaucoma and Secondary Neurodegeneration in the Brain

Glaucoma is one of the leading causes of irreversible blindness worldwide with a 2005 study conducted by (Allingham et al 2005) predicting that the condition affects more than 4 million Americans each year [24]. Glaucoma is a multifactorial neurodegenerative disorder where the eventual outcome is often blindness, first initiated with loss of peripheral vision followed by loss of central vision. The vision loss in glaucoma is attributed to cupping of the optic nerve head and subsequent thinning of the retinal nerve fibre layer (RNFL) thus causing RGC death and axonal degeneration. As RGC's are post mitotic neurons they have limited regenerative ability, hence neuroprotection is of utmost importance [25, 26].

The definition and diagnosis of glaucoma characterization is based on irido corneal angle morphology. As such, glaucoma can be classified into two broad categories: POAG (Primary Open Angle Glaucoma) and ACG (Angle Closure Glaucoma) with POAG being more common and prevalent [27, 28]. POAG is a slow progressive neurodegenerative disease that is characterised by; RGC degeneration, progressive visual field loss and concurrent cupping of the optic disk (See Figure 1-2). The above characteristics are the measurable progressive signs of the disease, however glaucoma is often also associated with increased intraocular pressure (IOP) and clinical management is aimed at reducing this pressure to and within a manageable limit which is known to slow down the disease process [28].

ACG however is more rapid and can progress to serious vision loss if it is not treated. These patients suffer from symptoms such as sudden blurred vision, headache, nausea and eye pain [29-31].

The vast majority of glaucoma sufferers worldwide suffer from POAG which is usually asymptomatic until the late stage of the disease where peripheral vision loss starts to become noticeable. Many patients report 'tunnel vision' during this stage. Reduced vision in turn leads to a poorer quality of life for the patient and added financial and mental burden on the patient and their family. Simple tasks such as driving, reading, watching television all become difficult, leading to a loss of independence [30].

Allingham et al (2005) predicted that 4 million people suffer from glaucoma in the United States. Recent epidemiological studies have shown glaucoma to be the second leading cause of blindness after cataract affecting more than 70 million people worldwide, with 2% of this sample size being around 40 years of age. Following continuing trends we can estimate the prevalence of glaucoma to reach 80 million people worldwide by 2020 [32, 33].

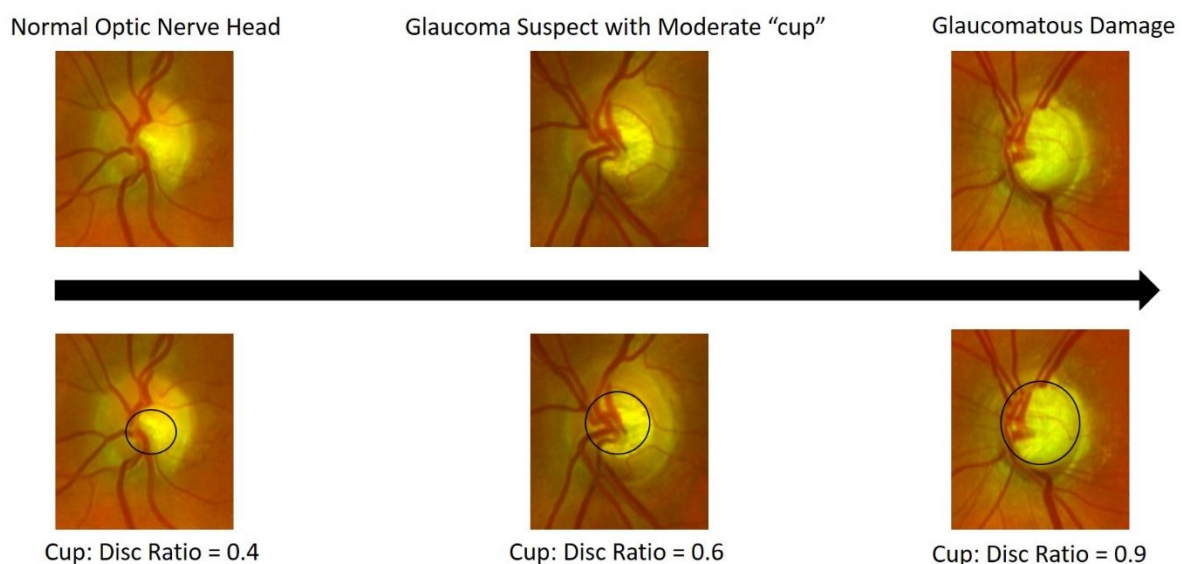


Figure 1-2. Range of Cup to Disc ratio (CDR).

Highlighting normal to glaucomatous damage as seen through *Optos UWF California (optomap colour)* of a dilated pupil with 1% mydriacyl. (Images taken by Samran Sheriff (Author) with Dr Jason Cheng (Glaucoma Specialist))

1.2.4. Risk factors and Clinical Management

The main observable diagnostic sign of glaucoma is elevated IOP. Clinically this elevated IOP is also a major risk factor. Normal IOP in humans range from 10-21 mmHg however, 25 - 50% of all glaucoma patients have pressure within this range and are referred to as normal tension glaucoma (NTG) [33]. Risk factors that predispose patients to glaucoma include; advancing age, low blood pressure, myopia and thin corneal thickness. Systemic risk factors include diseases such as diabetes mellitus, systemic hypertension, sleep apnoea and migraine headache [34, 35]. A strong family history together with a genetic component has also been established, suggesting that the diagnosis of glaucoma has a strong familial and genetic component [24]. Genetic studies since 2006 have identified gene variations in the MYOC, Cav1/Cav2 genes that might predispose a patient to develop glaucoma [36-38].

Current treatment in the management of glaucoma is aimed at reducing IOP to a suitable level as deemed by the medical practitioner, at which extra visual impairment is halted. Management involves the use of anti-glaucoma medications (prostaglandin analogues, beta blockers, carbonic anhydrase inhibitors and pilocarpine) applied topically to the affected eye in order to reduce pressure [39, 40]. If disease progression continues, surgical intervention such as; selective laser trabeculoplasty or trabeculectomy and in recent years the advancement of MIGS (micro-incisional glaucoma surgery) [41] can be offered to manage pressure and slow down RGC death and RNFL loss [31]. Despite available medical and surgical interventions, a number of patients still progress to end stage glaucoma and associated optic neuropathies. A 2007 study conducted by (Gupta 2007) proposed that IOP independent mechanisms may be at play in moderating RGC death and the degeneration associated with glaucoma progression. As such consideration and careful approach to monitoring IOP is no longer the only strategy used to protect RGCs [14].

1.2.5. Glaucoma and Neurodegeneration along the Optic Nerve

Recent literature has suggested that glaucoma is a neurodegenerative and trans synaptically mediated disease of the optic nerve and associated structures namely; LGN, optic radiations and visual cortex, with RGC death and ON damage the major pathological feature and major cause of irreversible vision loss in patients [42-45]. The phenomenon of neurodegeneration has been investigated in animal models of disease including AD and spinal cord diseases [46, 47] however, has provided little evidence overall to the hypothesis of glaucoma as a neurodegenerative condition. As previously discussed, the eye and retina remain extensions of the CNS, in the VP model anterograde (retina to visual cortex) and retrograde (visual cortex to retina) have been observed under various conditions with Wallerian degeneration in glaucoma remaining a critical focus in understanding the pathophysiology of the disease and its neuronal impact [48].

The precise mechanisms remain unknown however, induced oxidative damage and glutamate toxicity involvement has been proposed in TSD CNS injury in glaucoma. Axonal damage caused by oxidative stress leads to the damage of RGCs and has been thought to proceed the loss of cell bodies [49]. Trans synaptically this damage spreads to the LGN and visual cortex which induces RGC specific loss in areas of V1 and V2, eventually leading to damage of the entire posterior visual pathway [44]. The limits of this degeneration are currently not fully known, with recent findings by Keller et al (2014) [50] suggesting that RTSD does not extend beyond one synapsing neuron, with highly connecting interneurons preventing extension of the damage. It is this reason that has led to many hypothesizes and neuroprotective targets currently in development. The Akt pathway has been shown to offer neuroprotective properties on synaptic junctions and dendritic function [51] with a study by Cheng et al (2011) [52] reporting that Akt kinase supresses retrograde axonal degradation.

A reduction in IOP through medical or surgical means helps certain patients however, many signalling pathways are involved in RGC loss and are possible targets for therapy. In this thesis I have looked at elucidating the role of microstructural changes that develop via trans synaptic degeneration and will explore clinical methods to analyse its effects in glaucoma patients. Magnetic Resonance Imaging has shown atrophy in the LGN and visual cortex with Diffusion Tensor Imaging (DTI) showing altered diffusivity

measurements in the optic radiations/optic nerve of known glaucoma patients. The technique of DTI will be covered in more detail in the next chapter [53, 54].

1.3. Monitoring Neurodegenerative changes in the Visual Pathway

Non-invasive methods have been developed to demonstrate TSD in humans. Magnetic Resonance Imaging (MRI) is able to reveal optic nerve atrophy on T1 and T2 MRI sequences. OCT imaging of the RNFL may reveal thinning of the ganglion cell layer, Visual Field (VF) analysis is able to map field loss corresponding to ganglion cell death and DTI can be explored to assess markers of white matter integrity in RTSD and show microstructural white matter changes along the optic tract [55].

This chapter will explore the various methods available clinically to monitor neurodegenerative changes in the visual pathway.

1.3.1. Optical Coherence Tomography (OCT)

The advent of OCT in clinical practice has aided the management of glaucoma and has provided a new method to study TSD in the human visual system. Ganglion cell analysis on the OCT has allowed further subdivision of the retinal layers with completion in under five minutes per eye with guided progression analysis (See Figure 1-3 & 1-4). A study by Jindahra et al (2012) [67] showed that the rate of RNFL atrophy following occipital injury is 4.4um/year and that RNFL loss follows a logarithmic relationship between year of injury and degree of thinning. With a significant rate of RNFL loss each year monitoring neurodegenerative changes through various measures is critical to ensure stable progression.

A 2014 study conducted by Gabilondo et al (2014) [56], used OCT in a large cohort (n=100) with MS and found a strong correlation between loss of visual cortex volume and RNFL thinning. They found a 1cm³ loss of cortical volume correlated to a 0.6 reduction in RNFL thickness. Similarly, Petracca et al (2017) [68] performed a cross sectional analysis

comparing total macular volume and RNFL thickness with MRI in a (n=25) cohort of MS patients. RNFL thickness correlation against MRI was suggestive of TSD, while ganglion cell thickness was associated with cortical volume and lesion number.

1.3.2. Retinal Nerve Fibre Layer (RNFL) and Glaucoma

The early detection of glaucoma remains one of the most important challenges for specialists in order to limit damage and progression over time. RNFL analysis has been viewed as the benchmark of OCT imaging in glaucoma since its inception [58]. RNFL thickness analysis is used as an alternative to examine the neuroretinal rim as well as being used as a quantification measure in the estimation of retinal ganglion cell loss, helping to differentiate conditions such as myopia and physiological cupping. As a standalone test, RNFL thickness analysis has great diagnostic ability to detect early signs of glaucomatous damage [59, 60], when conducted on a spectral domain OCT (SDOCT) the reproducibility of RNFL thickness measurements is extremely high with intercorrelation of multiple measurements from a single individual greater than 96% accuracy [61] (See Figure 1-3 & 1-4).

Since retinal axons lack a myelin sheath until penetration occurs at the lamina cribrosa, the utilisation of OCT to image RNFL thickness is ideal for visualising neuroaxonal damage and understanding mechanisms of various brain disorders such as glaucoma. Vidal & Jordana (2012) found an inverse relationship between RNFL thickness and cerebral atrophy parameters using MRI imaging, thus concluding that decreased RNFL thickness might be used to predict brain activity [62, 63].

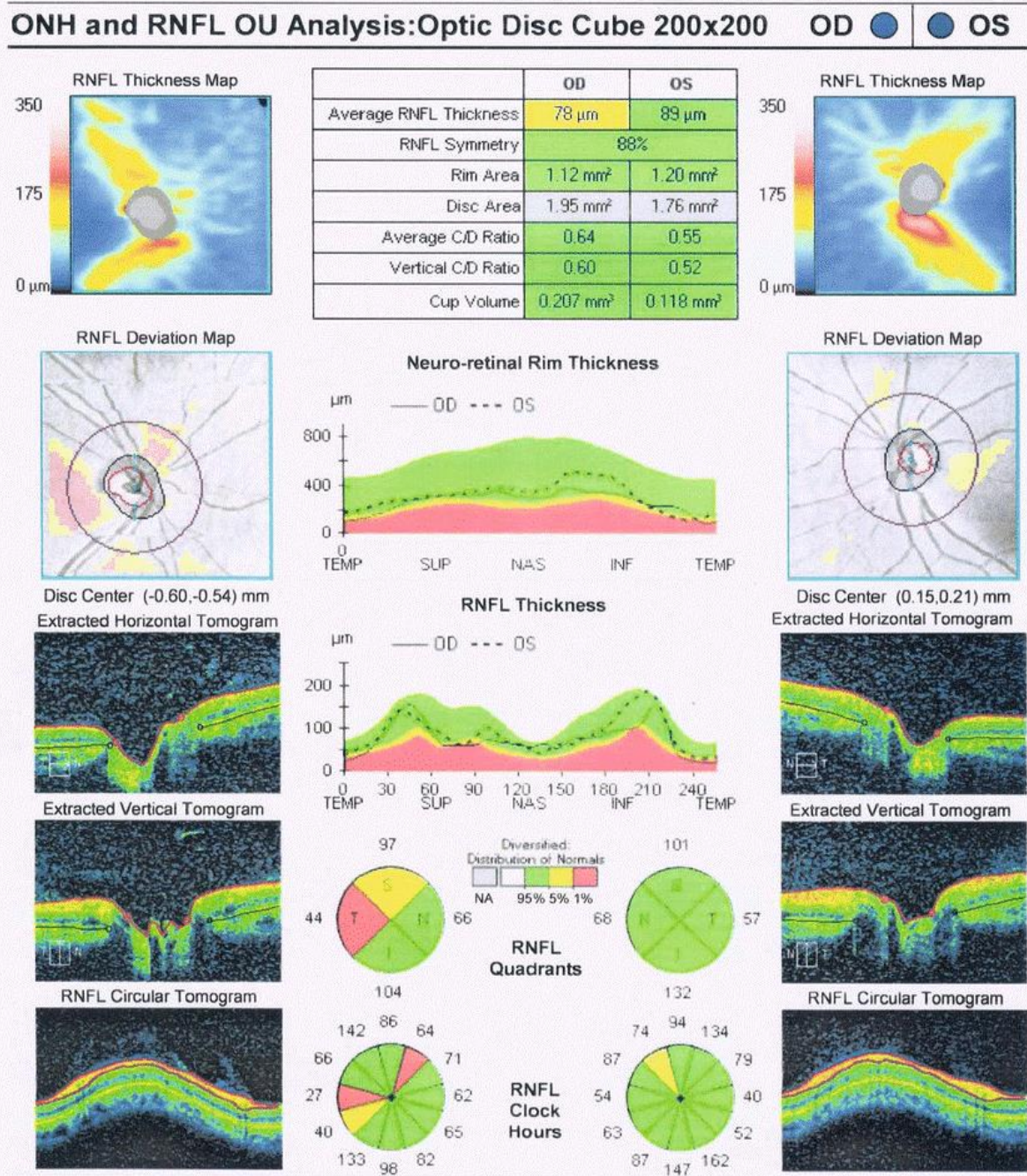


Figure 1-3. Optical Coherence Tomography (OCT) – Carl Zeiss OCT.

RNFL analysis report seen on Carl Zeiss OCT. ONH and RNFL OU analysis 200x200 report used to diagnose glaucomatous progression. RNFL thickness in the normal range is shown in green backgrounds, those that are abnormal at the 5% level are shown in yellow and those that are abnormal at the 1% level are shown in red backgrounds. (Images taken by Samran Sheriff (Author) with Dr Jason Cheng (Glaucoma Specialist). Image for Diagrammatic representation only.

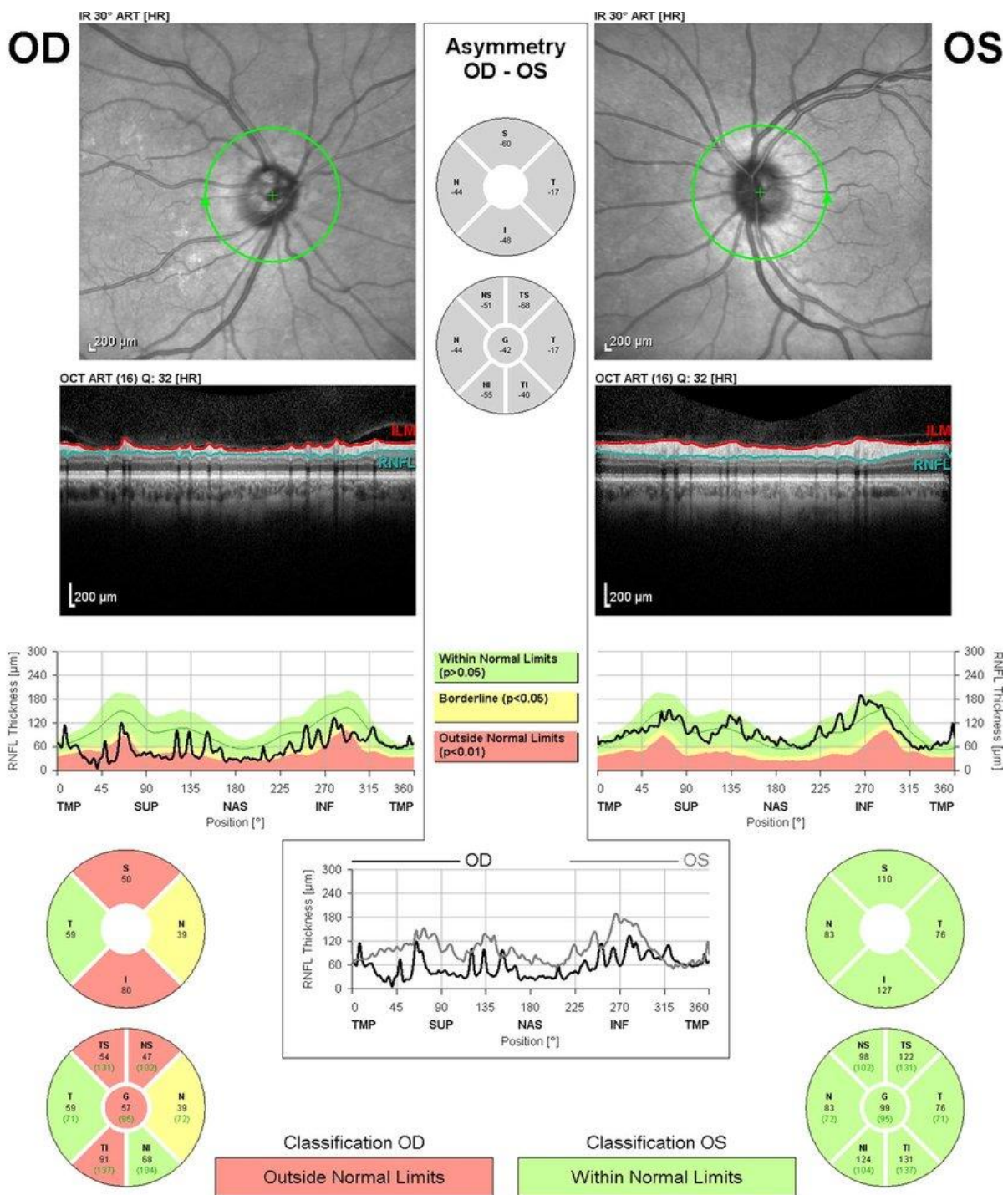


Figure 1-4. Optical Coherence Tomography (OCT) – Heidelberg OCT Spectralis.

RNFL analysis report seen on Heidelberg OCT Spectralis. ONH and RNFL OU with tracking laser tomography, used to diagnose glaucomatous progression. RNFL thickness in the normal range is shown in green backgrounds, those that are abnormal at the 5% level are shown in yellow and those that are abnormal at the 1% level are shown in red backgrounds.

(Images taken with permission from Prof. Stuart Graham, Principal Supervisor). Image for Diagrammatic representation only

1.3.3. Diffusion Tensor Imaging and Tractography

DTI provides a reliable non-invasive method to measure retrograde trans synaptic degeneration and has showed the greatest promise in present day neurology, as neurodegenerative conditions are best detected by analysing their measures of anisotropy and diffusivity [64, 65]. The principle behind the technique relies on the physiological movement of water molecules by a process known as diffusion from a certain point in vivo. Various pathological features of disease such as myelin, cell membranes and gliosis interfere with this apparent free movement of water and it is this value that is of importance clinically [64]. White matter tracts in the brain, are organised as bundles of axonal fibres running parallel along the direction of the tract, it is this structure that is used in diffusion anisotropy measurements. In theory, diffusion along the fibre is faster than perpendicular to the direction. Tractography is a 3D modelling technique that is used to visually represent the data collected through DTI. A variation to MRI imaging is used along with DTI computer-based imaging to present the results as 2D and 3D tractograms with colour coded DTMRI maps of white matter tracts in the brain created.

DTMRI has evolved as a non-invasive method to objectively predict the amount of white matter and associated pathologies with neuronal disease and allows assessment of therapeutic interventions at a much faster rate than conventional MRI techniques.

Table 1.1. Key MRI parameters measured during Diffusion Tensor Imaging of various neurological conditions.

MRI Parameter	Definition
Axial Diffusivity (AD)	λ_1 - Parallel Diffusivity – measure of water diffusion along the principal direction.
Radial Diffusivity (RD)	λ_{\perp} -Perpendicular Diffusivity – measure of water diffusion perpendicular to the principal direction.
Fractional Anisotropy (FA)	Degree of alignment of cellular structures within fibre tracts, and their structural integrity.
Mean Diffusivity (MD)	One third of the trace of the diffusion tensor, which is affected by cellular size and integrity.
Magnetization Transfer Ratio (MTR)	Capacity of the macromolecules in the CNS to exchange magnetization with the surrounding water molecules through dipole - dipole interactions.
T1 relaxation	The longitudinal decay constant for the recovery of the z component of the nuclear spin magnetization, towards its thermal equilibrium value.
T2 relaxation	The transverse decay constant for the recovery of M perpendicular to B
Myelin Water Imaging	Magnetic resonance method that provides an in vivo estimation of myelin content.

1.3.4. Visually Evoked Potential (VEP)

Visual evoked potential is the response that is measured from the occipital cortex in response to visual stimuli. Glaucoma being an eye disease characterised by optic neuropathy and characteristic visual field defects, it is well established that damage to RGC axons produces these noted defects. The question remains however the degree of apoptotic death and the possibility of neuroprotection once RGC death begins to occur. VEP is used in order to indicate the health of RGC axons by measuring their latency response. VEP is used to monitor neurodegeneration and evaluate visual function. Not routinely used in glaucoma management, VEP has the added benefit of being a non-invasive procedure and can be used as a measure of glaucomatous damage before RGC death occurs hence its use in TSD monitoring as a marker of reversible ganglion cell damage and an analysis measure of the integrity of the VP from ONH to V1.

1.3.5. Humphrey Visual Field (HVF)

HVF analysis of neurodegenerative conditions such as glaucoma has remained an invaluable clinical tool for detecting and monitoring visual function associated with glaucoma. Wu et al (2017) recently provided evidence-based guidance on the impact of testing frequency on the ability to detect the presence of visual field progression from evaluating a large longitudinal cohort of glaucoma participants, highlighting that the time required to detect progression was not proportionally reduced by increasing the number of tests performed per year. As smaller gains are achieved by increasing test frequency from twice to thrice yearly, a semi-annual testing routine in the first 2 years after diagnosis was suggested as acceptable to rule out rapid VF progression [60]. HVF in glaucoma treatment is performed every six months and compared with previous results to monitor progression and regression of the disease state. See Figure 1-5 for HVF 24-2 result highlighting glaucomatous progression.

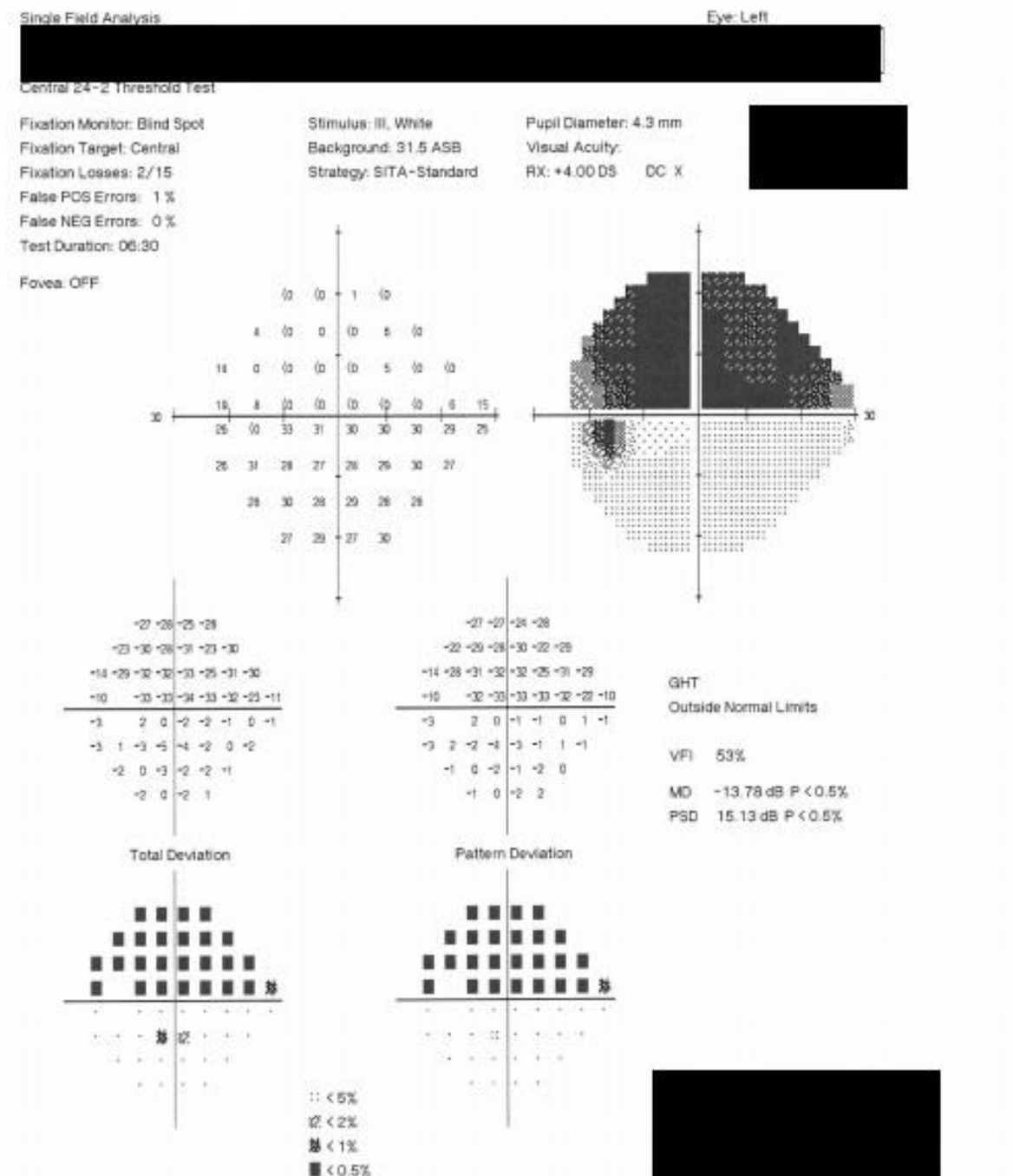


Figure 1-5 Humphrey Visual Field Analysis Left Eye OS- Glaucoma

Humphrey Visual Field Analysis 24-2 SITA FAST (Swedish Interactive Threshold Algorithm) used to analysis visual field loss relative to glaucomatous progression. (Images taken with permission from Prof. Stuart Graham, Principal Supervisor). Image for Diagrammatic representation only.

Table 1.2. Various Methods of MRI Myelin Quantification.

Method	Target	Advantages	Specificity for Myelin
Conventional (MRI)	Myelin	<ul style="list-style-type: none"> • Routinely used in neurological cases • High spatial resolution and anatomical definition 	Low
Magnetization Transfer Ratio (MTR)	Myelin	<ul style="list-style-type: none"> • Reasonable acquisition times • High precision and simple post acquisition processing algorithm 	Moderate
Diffusion Tensor Imaging (DTI)	Myelin	<ul style="list-style-type: none"> • Potential to distinguish pure demyelination, axonal damage or both within T2 hyper intensive lesions • Evaluate changes and disability over time 	Low
Myelin Water Fraction (MWF)	Myelin	<ul style="list-style-type: none"> • High specificity for myelin • Good intrasite and intersite reliability and reproducibility across platforms 	High
VEP Latency (VEP)	Myelin	<ul style="list-style-type: none"> • Highly sensitive for diagnosis of anterior VP abnormalities • Ideal for visualising neuroaxonal damage 	Moderate

1.4. Hypothesis and Research Plan

This project aims to use the visual pathway as a model to explore neurodegenerative diseases and thus, monitor acute and chronic factors that play a role in injury and repair within the CNS.

In effect, the hypothesis being tested will be accomplished by conducting a comprehensive post-mortem meta-analysis, which will be able to determine through correlation analysis which MRI parameter is directly responsible for measuring demyelination, a concept which has not been addressed previously.

This study will also employ DTI imaging in order to understand microstructural changes in the posterior visual pathway in glaucoma patients in order to delineate neurodegeneration in glaucoma, followed by a comprehensive analysis comparing adjusted retinal nerve fibre layer (RNFL) thickness and MRI parameter values in the visual pathway. As such I hypothesise, based on previous studies from my research group and extensive literature analysis (Paper 1), that radial diffusivity (RD) will be the best predictor of demyelination in post mortem brain samples. I hypothesise that the magnetization transfer ratio (MTR) will be the best predictor of demyelination out of the additional variables measured.

Addressing the following aims will test this hypothesis

1. Which MRI parameters are measuring demyelination in the brain?
2. Whether demyelination is the initial pathological change in glaucoma.

1.5. References

1. Chiba, T., Nishimoto, I., Aiso, S. and Matsuoka, M., , Neuroprotection against neurodegenerative diseases. *Molecular neurobiology*, 2007. **35(1)**: p. p.55.
2. Vanzetta, I. and A. Grinvald, Coupling between neuronal activity and microcirculation: implications for functional brain imaging. *HFSP J*, 2008. **2(2)**: p. 79-98.
3. Stein, B.E. and B.A. Rowland, Organization and plasticity in multisensory integration: early and late experience affects its governing principles. *Prog Brain Res*, 2011. **191**: p. 145-63.
4. London, A., I. Benhar, and M. Schwartz, The retina as a window to the brain-from eye research to CNS disorders. *Nat Rev Neurol*, 2013. **9(1)**: p. 44-53.
5. De Groef, L. and M.F. Cordeiro, Is the Eye an Extension of the Brain in Central Nervous System Disease? *J Ocul Pharmacol Ther*, 2018. **34(1-2)**: p. 129-133.
6. Marner, L., et al., Marked loss of myelinated nerve fibers in the human brain with age. *J Comp Neurol*, 2003. **462(2)**: p. 144-52.
7. Jellison, B.J., Field, A.S., Medow, J., Lazar, M., Salamat, M.S. and Alexander, A.L.,, Diffusion tensor imaging of cerebral white matter: a pictorial review of physics, fiber tract anatomy, and tumor imaging patterns. *American Journal of Neuroradiology*,, 2004. **25(3)**: p. pp.356-369.
8. Lawlor, Mitchell, Helen Danesh-Meyer, Leonard A. Levin, Indran Davagnanam, Enrico De Vita, and Gordon T. Plant. "Glaucoma and the brain: trans-synaptic degeneration, structural change, and implications for neuroprotection." *Survey of ophthalmology* 63, no. 3 (2018): 296-306.
9. Patel.KR, et al., Early diffusion evidence of retrograde transsynaptic degeneration in the human visual system. *Neurology*, 2016(Jun).
10. You, Y., et al., Demyelination precedes axonal loss in the transneuronal spread of human neurodegenerative disease. *Brain*, 2019. **142(2)**: p. 426-442.
11. Ptito, A. and S.E. Leh, Neural substrates of blindsight after hemispherectomy. *Neuroscientist*, 2007. **13(5)**: p. 506-18.
12. Herbin, M., Boire, D., Théoret, H. and Ptito, M.,, Transneuronal degeneration of retinal ganglion cells in early hemispherectomized monkeys. . *Neuroreport*, 1999. **10(7)**: p. pp.1447-1452.
13. Su, J.H., Deng, G. and Cotman, C.W., 1997, Transneuronal degeneration in the spread of Alzheimer's disease pathology: immunohistochemical evidence for the transmission of tau hyperphosphorylation. *Neurobiology of disease*, 1997.: p. 365-375.

14. Gupta, N.a.Y., Y.H., Glaucoma as a neurodegenerative disease. . Current opinion in ophthalmology, 2007. **18(2)**: p. pp.110-114.
15. Shen, T., et al., Differing Structural and Functional Patterns of Optic Nerve Damage in Multiple Sclerosis and Neuromyelitis Optica Spectrum Disorder. Ophthalmology, 2019. **126(3)**: p. 445-453.
16. Costello, F., The afferent visual pathway: designing a structural-functional paradigm of multiple sclerosis. ISRN Neurol, 2013. **2013**: p. 134858.
17. Zhou, W., et al., MRI Study of the Posterior Visual Pathways in Primary Open Angle Glaucoma. J Glaucoma, 2017. **26(2)**: p. 173-181.
18. Grill-Spector, K.a.M., R., The human visual cortex. Annu. Rev. Neurosci., 2004. **27**,: p. pp.649-677.
19. DiCarlo, J.J., D. Zoccolan, and N.C. Rust, How does the brain solve visual object recognition? Neuron, 2012. **73(3)**: p. 415-34.
20. Miller, D.H., Biomarkers and surrogate outcomes in neurodegenerative disease: lessons from multiple sclerosis. NeuroRx, 2004. **1(2)**: p. pp.284-294.
21. Glass, C.K., et al., Mechanisms underlying inflammation in neurodegeneration. Cell, 2010. **140(6)**: p. 918-34.
22. Green, A.J., et al., Ocular pathology in multiple sclerosis: retinal atrophy and inflammation irrespective of disease duration. Brain, 2010. **133(Pt 6)**: p. 1591-601.
23. Efendi, H., Clinically Isolated Syndromes: Clinical Characteristics, Differential Diagnosis, and Management. Noro Psikiyatr Ars, 2015. **52(Suppl 1)**: p. S1-S11.
24. Allingham, R.R., Y. Liu, and D.J. Rhee, The genetics of primary open-angle glaucoma: a review. Exp Eye Res, 2009. **88(4)**: p. 837-44.
25. Weber, A.J.a.H., C.D, Structure–function relations of parasol cells in the normal and glaucomatous primate retina. . Investigative ophthalmology & visual science,, 2005. **46(9)**: p. pp.3197-3207.
26. Cheung, W., L. Guo, and M.F. Cordeiro, Neuroprotection in glaucoma: drug-based approaches. Optom Vis Sci, 2008. **85(6)**: p. 406-16.
27. Lee, D.A.a.H., E.J.,, Glaucoma and its treatment: a review. American journal of health-system pharmacy,. American journal of health-system pharmacy,, 2005. **62(7)**: p. pp.691-699.
28. Kwon, Y.H., et al., Primary open-angle glaucoma. N Engl J Med, 2009. **360(11)**: p. 1113-24.
29. Wright, C., Tawfik, M.A., Waisbourd, M. and Katz, L.J., Primary angle-closure glaucoma: an update. . Acta ophthalmologica, 2016. **94(3)**: p. pp.217-225.

30. Weinreb, R.N. and P.T. Khaw, Primary open-angle glaucoma. *The Lancet*, 2004. **363**(9422): p. 1711-1720.
31. Weinreb, R.N., T. Aung, and F.A. Medeiros, The pathophysiology and treatment of glaucoma: a review. *JAMA*, 2014. **311**(18): p. 1901-11.
32. Quigley, H.A., Number of people with glaucoma worldwide. *British journal of ophthalmology*, 1996. **80**(5): p. pp.389-393.
33. Quigley, H.A. and A.T. Broman, The number of people with glaucoma worldwide in 2010 and 2020. 2006. **90**(3): p. 262-267.
34. Hewitt, A.W., et al., A Glaucoma Case-control Study of the WDR36 Gene D658G sequence variant. *Am J Ophthalmol*, 2006. **142**(2): p. 324-5.
35. Ishikawa, M., et al., Risk factors for primary open-angle glaucoma in Japanese subjects attending community health screenings. *Clin Ophthalmol*, 2011. **5**: p. 1531-7.
36. Kumar, A., Basavaraj, M.G., Gupta, S.K., Qamar, I., Ali, A.M., Bajaj, V., Ramesh, T.K., Prakash, D.R., Shetty, J.S. and Dorairaj, S.K., Role of CYP1B1, MYOC, OPTN and OPTC genes in adult-onset primary open-angle glaucoma: predominance of CYP1B1 mutations in Indian patients. *Molecular vision*, 2007. **13**: p. 667.
37. Wiggs, J.L., et al., Common variants near CAV1 and CAV2 are associated with primary open-angle glaucoma in Caucasians from the USA. *Hum Mol Genet*, 2011. **20**(23): p. 4707-13.
38. Mookherjee, S., Acharya, M., Banerjee, D., Bhattacharjee, A. and Ray, K., Molecular basis for involvement of CYP1B1 in MYOC upregulation and its potential implication in glaucoma pathogenesis. . *PloS one*, 2012. **7**(9): p. p.e45077.
39. Cheema, A., et al., Update on the Medical Treatment of Primary Open-Angle Glaucoma. *Asia Pac J Ophthalmol (Phila)*, 2016. **5**(1): p. 51-8.
40. Conlon, R., H. Saheb, and Ahmed, II, Glaucoma treatment trends: a review. *Can J Ophthalmol*, 2017. **52**(1): p. 114-124.
41. Bloom, P. and L. Au, "Minimally Invasive Glaucoma Surgery (MIGS) Is a Poor Substitute for Trabeculectomy"-The Great Debate. *Ophthalmol Ther*, 2018.
42. Yücel, Y.H., et al., Effects of retinal ganglion cell loss on magno-, parvo-, koniocellular pathways in the lateral geniculate nucleus and visual cortex in glaucoma. . *Progress in retinal and eye research*, 2003. **22**: p. 465-81.
43. Zhang, Y., et al., Pathological correlates of magnetic resonance imaging texture heterogeneity in multiple sclerosis. *Annals of Neurology*, 2013. **74**(1): p. 91-99.
44. de Calignon, A., et al., Propagation of tau pathology in a model of early Alzheimer's disease. *Neuron*, 2012. **73**(4): p. 685-697.

45. Di Polo, A., Aigner, L.J., Dunn, R.J., Bray, G.M. and Aguayo, A.J., Prolonged delivery of brain-derived neurotrophic factor by adenovirus-infected Müller cells temporarily rescues injured retinal ganglion cells. *Proceedings of the National Academy of Sciences*, 1998. **95**(7): p. 3978-3983.
46. Ginsberg, S.D.a.M., L.J., Axonal transection in adult rat brain induces transsynaptic apoptosis and persistent atrophy of target neurons. *Journal of neurotrauma*, 2002. **19**(1): p. pp.99-109.
47. Canudas, A.M., et al., Endogenous brain-derived neurotrophic factor protects dopaminergic nigral neurons against transneuronal degeneration induced by striatal excitotoxic injury. *Brain Res Mol Brain Res*, 2005. **134**(1): p. 147-54.
48. Quigley, H.A. and A.T. Broman, The number of people with glaucoma worldwide in 2010 and 2020. *Br J Ophthalmol*, 2006. **90**(3): p. 262-7.
49. Howell, G.R., et al., Intrinsic axonal degeneration pathways are critical for glaucomatous damage. *Exp Neurol*, 2013. **246**: p. 54-61.
50. Johannes Keller, B.F.S.n.-D., Pablo Villoslada, Lesions in the Posterior Visual Pathway Promote TransSynapticDegeneration of Retinal Ganglion Cells. 2014.
51. Duarte, A.I., et al., Insulin neuroprotection against oxidative stress is mediated by Akt and GSK-3beta signaling pathways and changes in protein expression. *Biochim Biophys Acta*, 2008. **1783**(6): p. 994-1002.
52. Cheng, H.C., et al., Akt suppresses retrograde degeneration of dopaminergic axons by inhibition of macroautophagy. *J Neurosci*, 2011. **31**(6): p. 2125-35.
53. Schmierer, K., et al., Quantitative magnetic resonance of postmortem multiple sclerosis brain before and after fixation. *Magnetic resonance in medicine*, 2008. **59**(2): p. 268-277.
54. Schmierer, K., et al., Diffusion tensor imaging of post mortem multiple sclerosis brain. *NeuroImage*, 2007. **35**(2): p. 467-477.
55. Dinkin, M., Trans-synaptic Retrograde Degeneration in the Human Visual System: Slow, Silent, and Real. *Curr Neurol Neurosci Rep*, 2017. **17**(2): p. 16.
56. Gabilondo, I., et al., Trans-synaptic axonal degeneration in the visual pathway in multiple sclerosis. *Ann Neurol*, 2014. **75**(1): p. 98-107.
57. Laule, C., et al., Myelin water imaging in multiple sclerosis: quantitative correlations with histopathology. *Multiple Sclerosis Journal*, 2006. **12**(6): p. 747-753.
58. Huang, D., et al., Optical coherence tomography. *Science (New York, N.Y.)*, 1991. **254**(5035): p. 1178-1181.

59. Mwanza, J.-C., et al., Ability of cirrus HD-OCT optic nerve head parameters to discriminate normal from glaucomatous eyes. *Ophthalmology*, 2011. **118**(2): p. 241-8.e1.
60. Wu, Z., et al., Frequency of Testing to Detect Visual Field Progression Derived Using a Longitudinal Cohort of Glaucoma Patients. *Ophthalmology*, 2017. **124**(6): p. 786-792.
61. Mwanza, J.-C., et al., Reproducibility of peripapillary retinal nerve fiber layer thickness and optic nerve head parameters measured with cirrus HD-OCT in glaucomatous eyes. *Investigative ophthalmology & visual science*, 2010. **51**(11): p. 5724-5730.
62. Galetta, K.M., et al., Optical coherence tomography (OCT): imaging the visual pathway as a model for neurodegeneration. *Neurotherapeutics : the journal of the American Society for Experimental NeuroTherapeutics*, 2011. **8**(1): p. 117-132.
63. Kallenbach, K. and J. Frederiksen, Optical coherence tomography in optic neuritis and multiple sclerosis: a review. 2007. **14**(8): p. 841-849.
64. Le Bihan, D., Looking into the functional architecture of the brain with diffusion MRI. *Nature Reviews Neuroscience*, 2003. **4**: p. 469.
65. Le Bihan, D., Mangin, J.F., Poupon, C., Clark, C.A., Pappata, S., Molko, N. and Chabriet, H., , Diffusion tensor imaging: concepts and applications. *Journal of Magnetic Resonance Imaging. An Official Journal of the International Society for Magnetic Resonance in Medicine*, 2001. **13**(4): p. pp.534-546.
66. Van Buren, J.M, Trans-synaptic retrograde degeneration in the visual system of primates. *Journal of neurology, neurosurgery, and psychiatry*, 1963. **26**(5): p. 402.
- 67 Jindahra, P., Petrie, A. and Plant, G.T, The time course of retrograde trans-synaptic degeneration following occipital lobe damage in humans. *Brain*, 2012. **135**(2): p. 534-541
68. Petracca, M., Cordano, C., Cellerino, M., Button, J., Krieger, S., Vancea, R., Ghassemi, R., Farrell, C., Miller, A., Calabresi, P.A. and Lublin, F., Retinal degeneration in primary-progressive multiple sclerosis: a role for cortical lesions? *Multiple Sclerosis Journal*, 2017. **23**(1): p. pp 43-50

2. Association between Studies

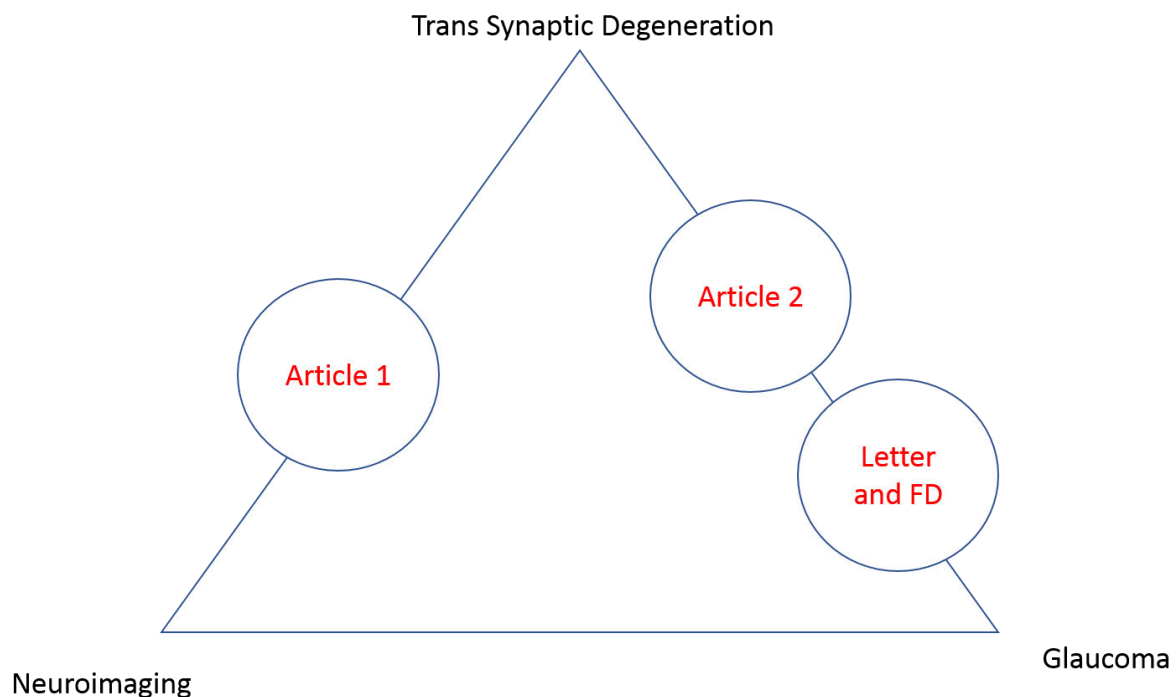


Figure 2-1. Position of Individual articles (Paper 1 & Paper 2) within various thematic areas.

A recent hypothesis to enter the literature alludes to glaucoma as a neurodegenerative disease, the basis for this finding has been drawn from central nervous system changes in glaucoma patients seen through histology and neuroimaging. The idea for glaucoma to be considered a neurodegenerative condition relies on the complex interplay of trans synaptic degenerative changes as well as confirmation through neuroimaging (See Figure 2-1). It is known that RGC cell loss leads to anterograde and retrograde degeneration as well as TSD which is a hallmark feature of a range of other optic neuropathies such as optic neuritis. Recently similar studies have confirmed these microstructural changes using neuroimaging techniques of diffusion imaging.

This thesis aims to elucidate the notion of 'glaucoma as a neurodegenerative disease' through clinical (Paper 2) and analytical research (Paper 1) within various thematic areas, underlying trans synaptic degeneration in glaucoma. Further research will be required to identify brain changes in glaucoma which may have critical implications for neuroprotection and future treatment strategies in addition to our current understanding of glaucoma (Future Directions).

3. Quantification of MRI parameters against demyelination in the white matter: A systematic analysis of post mortem quantitative imaging and histopathological studies

SHERIFF, S., KLISTORNER, A., GUPTA, VK., GRAHAM, SL., YOU, YUYI. 2018. Quantification of MRI parameters against demyelination and axonal loss in the white matter: A systematic analysis of post mortem quantitative imaging and histopathological studies. (*Intended Journal for Review/Publication - Neurology*)

3.1. Abstract

Objective - To investigate the association between MRI parameters and demyelination within the white matter of the central nervous system.

Methods – Histological studies were gathered from PubMed and Web of Science that evaluated myelin loss using post mortem quantitative imaging and histopathological analysis. Key terms for searching included (Postmortem or Post-Mortem) AND (MRI) AND (Demyelination).

MRI parameters analysed included; fractional anisotropy (FA), mean diffusivity (MD), radial diffusivity (RD), axial diffusivity (AD), magnetization transfer ratio (MTR), T1/ T2 relaxation time and myelin water imaging (MWI). Statistical analysis included a weighted pooled random effects model for correlation between either Axonal loss (AL) / Myelin loss (ML) and one of the above parameters.

Results - 626 articles were identified from the literature with fifteen fulfilling the inclusive criteria. In total, 1983 Region of Interest (ROI) were analysed from 178 subjects (83 female and 21 male). Samples were taken from either post mortem brains or spinal cords. MTR was overall the best predictor of both demyelination ($r=-0.732$ 95% CI: -0.787 - -0.667 $p<0.001$) and axonal loss ($r=-0.666$ 95% CI: -0.758--0.547, $p<0.001$). Of all the diffusivity measures, RD showed the strongest correlation with myelin loss; ($r=0.747$ 95% CI: 0.601- 0.845, $p<0.001$) followed by MD, FA and AD. FA ($r=-0.634$ 95%CI: -0.704- -

0.552, $p < 0.001$) was the best diffusivity predictor of axonal loss. Myelin water fraction (MWF) also exhibited a moderate correlation with myelin density ($r = 0.49$) from calculated values.

Conclusion – MTR was overall the best predictor of both demyelination and axonal loss. Of all the diffusivity indices, RD demonstrated the strongest association with demyelination. The association of MRI parameters against myelin loss was overall stronger than the association with axonal loss.

3.2. Introduction

Multiple Sclerosis (MS) is an inflammatory, demyelinating and neurodegenerative disease of the central nervous system. Focal demyelination and axonal loss are the most characteristic pathological changes that occur in multiple sclerosis and are thus important signs for clinically monitoring and evaluating the progression of the disease [1]. Throughout the progression of the disease significant attempts have been made to visualise and monitor histological changes than solely using MRI. Myelin loss (ML) and axonal loss (AL) are two characteristic microstructural changes that progress throughout the course of the disease and have thus proved useful markers for measuring and monitoring the condition using neuroimaging techniques [2]. Myelin Water Imaging (MWI) has arisen as a new technique to quantitatively define the role of myelin specific pathology and MS pathogenesis and aims to be invaluable in understanding neurological disorders [3].

Current MRI measurements that have shown promise in measuring demyelination and axonal loss are not only limited to MS clinical trials but have also shown promise in various central nervous system diseases; Alzheimer's disease (AD) [4], Parkinson's disease [5] and Stroke [6]. These include diffusivity measures and magnetization transfer ratio (MTR). The exact mechanism that governs brain diffusivity has not yet been fully understood, however diffusion characteristics have suggested that radial diffusivity (RD) to be a promising biomarker for measurement of myelination [2]. Experimental work using RD as a measure of demyelination has yielded a strong relationship when comparing myelin loss and measurements in RD [7]. Post mortem human studies of MS patients have revealed increased levels of RD in brain regions that showed increased demyelination [2, 8] whilst

similar work in animal models has shown that directional diffusivity measures (RD and AD) to be a reliable method of myelin quantification in the CNS [9]. There has also been conflicting evidence with RD and measures of demyelination with one study failing to show a positive relationship between an increase in RD and level of demyelination, suggesting that the association may not be pathologically specific, leaving the answer still unknown [10].

The first correspondence between Myelin Water Imaging and myelin density was observed by Moore et al (2000) who showed qualitative distribution between myelin water and Luxol fast blue (LFB) a histological marker for myelin, thus providing evidence that (MWI) could be used as an accurate in vivo marker of myelin content along with MRI parameters and diffusivity measures [11].

The purpose of this study is therefore to explore all available MRI diffusion parameters in central nervous system diseases in order to identify which parameter is the best measure of demyelination and axonal loss. The findings of this systemic review are likely to be beneficial for monitoring progression of neurodegenerative diseases.

3.3. Methods

3.3.1. Overview of Review Method

The primary objective of this study was to identify which MRI parameter is the best predictor of demyelination and axonal loss. We compared each of the four key parameters (MD, AD, RD, FA) as well as MTR, T1/T2 Relaxation Time and MWF between various reported histological studies and against either ML (Myelin Loss) and AL (Axonal Loss). This review was performed and adheres to the Preferred Reporting Items for Systematic Reviews and adheres to (PRISMA) methodology for study selection. (See Figure 3-3) for PRISMA flow diagram of included studies.

In addition, this study also adheres to the Moose Guidelines for Meta – Analyses and Systematic Reviews of Observational Studies.

3.3.2. Data sources and Chosen Search Strategy

An electronic online database search was chosen as the primary data collection method. The following databases were searched: PubMed and Web of Science. Search terms

used for identification included: (Postmortem or Post-Mortem) AND (MRI) and (Demyelination).

Search strategies for each individual database are available and included in (Appendix 1). We also manually reviewed the reference lists from articles identified through the database search and identified additional relevant studies for inclusion. All studies that included a post mortem protocol were considered for inclusion in this review. Knowing that post mortem clinical studies are seldom conducted, a large number of articles were excluded during the searching process leaving only a small number of suitable articles for inclusion. Inclusion criteria consisted of: (1) English language articles, (2) Histological post mortem analysis i.e. myelin and axonal staining, (3) study conducted between 2002 – 2017, (4) Using DTI (Diffusion Tensor Imaging) analysis. Studies were excluded if any of the following criteria were found: (1) Study conducted in animal models of disease, (2) Studies lacking quantitative analysis, (3) Neurological studies not exploring MRI parameters.

3.3.3. Study Selection

Data from each included study was extracted and extrapolated by the investigator (S.S). Two levels of screening were applied, first a broad screening protocol applying the inclusion criteria was performed by reading the abstract and studies were either deemed 'Relevant' or 'Irrelevant'. For all articles deemed relevant the second screening method was followed by reviewing the article in full and extrapolating; name of the first author, publication year, region of interest (ROI)/ sample size, number of participant (case/control), Tissue preparation technique, disease type, Included MRI parameters; ML value and AL value. Any clarification and disputes regarding relevance were discussed by the co-authors and clarified. (See Table 3-1) for included study characteristics and (Figure 3-3) for PRISMA flow diagram of included studies.

3.3.4. Data Extraction and Quality Assessment

In order to assess the quality and diagnostic accuracy of studies included, (QUADAS-2) version 2 was used. The study tool was chosen in order to assess the quality of data included in review.

The QUADAS -2 assessment involved four areas. 1) Patient Selection, 2) Index Tests, 3) Reference Standard, 4) Flow of patients. Each key area was analysed across the fifteen

studies to assess risk of bias. Methodological quality of all studies was relatively high in accordance with QUDAS-2.

In one study which did not specify ROI examined [12], data points were counted in scatterplot graphs to determine total number of ROI for analysis.

Appendix 4 provided by request for QUADAS-2 assessment raw data.

3.3.5. Statistical Methods

Statistical Analysis for this review was completed using MedCalc (Medcalc Software package version 18.10.12, Ostend, Belgium) [13-15]. The outcome was a correlation analysis between MRI parameters and either (ML) or (AL).

Key data from each study including (ML) and (AL) values as well as total region of Interest (ROI) explored in each study were pooled into a weighted summary. In those studies that explored a range of ROI, a mean ROI value was used for statistical analysis. Relative risks with 95% CI interval were analysed to determine the relationship between an individual MRI parameter and either AL or ML using a random effects model since individual studies varied in effect size due to the likelihood of study heterogeneity in terms of DTI techniques, subject tissue preparation and analysis (See Figure 3-1 & 3-2).

3.4. **Results**

3.4.1. Identification and Selection of Studies

Records identified through database searching yielded 626 articles using the keywords (Postmortem or Post-Mortem) AND (MRI) and (Demyelination). Articles were screened by reading the title/abstract only and applying inclusion criteria. Thirteen articles were retrieved by the reviewers from the original 626 identified [2, 3, 8, 12, 16-24]. We also manually reviewed the reference lists from articles identified through the database search and identified two additional relevant studies for inclusion based on the inclusion criteria mentioned prior that failed to appear in the initial literature search [25, 26]. (See Figure 3-3) for PRISMA flow diagram of included studies).

3.4.2. Study Characteristics and Geographic Distribution

In total 1983 Region of Interest (ROI) were analysed from 178 subjects. Of the fifteen studies selected, only ten reported the gender of samples included totalling (83 female and 21 male) post mortem samples from either brains or spinal cords. Geographical distribution of included studies included (four in America, two in Europe, seven from the United Kingdom and two from Canada).

3.4.3. Correlation between MRI parameters and variables against either (ML/AL)

Statistical analysis of included studies for (ML) revealed T2 relaxation time and MTR to have the strongest correlation with myelin loss. T2 relaxation time was observed to have the best correlation against myelin loss ($r=0.774$ 95%CI: 0.645 - 0.860, $p<0.001$) followed by MTR ($r=-0.732$ 95% CI: -0.787 - -0.667 $p<0.001$). T1 relaxation time was also positively correlated with myelin loss ($r=0.725$ 95%CI: 0.606 - 0.813 $p<0.001$). Correlation against key diffusivity markers revealed radial diffusivity (RD) as the best predictor of myelin loss ($r=0.747$ 95% CI: 0.601 - 0.845, $p<0.001$) followed by FA ($r= -0.650$ 95% CI: -0.771- -0.486, $p<0.001$), MD ($r= 0.647$ 95% CI: 0.496 - 0.760, $p<0.001$), and AD ($r=0.610$ 95% CI: 0.303 - 0.800, $p<0.001$). (See Figure 3-1) for individual correlation.

Statistical analysis of included studies revealed MTR as the best overall predictor of axonal loss ($r=-0.666$ 95% CI: 0.758 - 0.547, $p<0.001$). T1/T2 relaxation time were able to show better predictors of change in axonal loss compared to diffusivities, T1 ($r=0.633$ 95%CI: 0.533 - 0.715, $p<0.001$) and T2 ($r=0.680$ 95%CI: 0.481 – 0.812, $p <0.001$). Correlation against key diffusivity markers revealed FA ($r=-0.634$ 95%CI: -0.704 - -0.552, $p<0.001$) to have the highest r value followed by MD ($r=0.561$,95%CI: 0.456 – 0.651, $p<0.001$) , RD ($r=0.553$, 95%CI: 0.430 – 0.656, $p<0.001$) and AD ($r=0.548$, 95% CI: 0.426 – 0.651, $p<0.001$). (See Figure 3-2) for individual correlation.

Myelin water fraction (MWF) also exhibited a moderate correlation with myelin density ($r=0.49$) from calculated values obtained in the following studies [3, 24].

Statistical analysis revealed that the association between MRI diffusion parameters was overall stronger when compared against (ML) as opposed to (AL). Table 3-2 shows correlation values between each individual MRI parameter against (ML) and (AL). MTR was strongly associated with both axonal loss and demyelination and revealed the highest correlation when compared to the diffusion parameters. Correspondingly the same result was observed in RD as hypothesised which showed a strong association with an increase in the level of demyelination.

Table 3.1. Demographic Data of studies included in Analysis.

Study and Disease Type	n	Staining Technique	Disease Type	MRI Parameters Tested
1. Schmierer et al. (2008)	47-66 (ROI); 15 (P)	LFB/Cres Violet BIEL; (fi/fr)	MS	MD, AD, RD, FA, T1, T2, MTR
2. Schmierer et al. (2007)	44-51 (ROI); 16 (P)	LFB, GFAP, BIEL, H&E (fr)	MS	MD, FA
3. Seewan et al. (2009)	42 (ROI); 10 (P)	LFB, H&E, BS, GFAP (fi)	MS	FA, T1, T2, MTR
4. Moll et al. (2012)	48 (ROI); 4 (P)	MBP, nf (fi)	MS	MD, AD, RD, FA, MTR
5. Schmierer et al. (2004)	63-72 (ROI); 20 (P)	LFB, H&E, BIEL, GFAP (fr)	MS	T1, MTR
6 Guow et al. (2008)	104 (ROI); 18 (P)	LFB, H&E, BIEL, GFAP (fi)	AD	FA, T1
7. Bot et al. (2004)	158 (ROI); 11 (P)	Kluver (myelin), NE-14 PN (axons) (fi)	MS	T1, T2, MTR
8. Mottershead et al. (2003)	108 (ROI); 5 (P)	LFB/Cres Violet BIEL; (fi)	MS	T1, T2, MTR
9. Kolasinski et al. (2012)	35 (ROI); 9 (P)	APPL, PS, LFB/Cres; (fi)	MS	MD, FA
10. Wang et al. (2014)	42 ROI; 3 (P)	LFB- (PAS), H&E, BIEL, (fi)	MS	AD, RD, MTR
11. Schmierer et al. (2009)	21-25 ROI; 21 (P)	LFB/Cres Violet H&E; (fi)	MS	T1,T2
12. Van der Voorn et al. (2011)	55 ROI; 20 (P)	LFB, BS, GFAP (fi)	X –ALD	MTR, FA
13. Fisher et al. (2007)	110 ROI; 10 (P)	PLP; (fi)	MS	MTR, T1
14. Laule et al. (2008)	22-30 ROI /Sample; 3 (P)	LFB; (fi)	MS	MWF
15. Laule et al. (2006)	23-45 ROI / Sample; 13 (P)	LFB; (fi)	MS	MWF

Abbreviations:

MD = Mean Diffusivity, FA = Fractional Anisotropy, AD = Axial Diffusivity, RD = Radial Diffusivity, MTR = Magnetization Transfer Ratio, T1 Relaxation Time, T2 Relaxation Time, MWF = Myelin Water Fraction
H&E= Haematoxylin and Eosin, LFB= Luxol fast Blue, LFB PAS = Luxol Fast Blue – Periodic Acid Schiff , Cres= Cresyl Violet , BIEL = Bielschowsky silver , GFAP= Glial fibrin acidic protein , PN= phosphorylated neurophilaments, BS= Bodian Silver, PS = Palmgren Silver, APPL = Anti proteolipid , MBP = Myelin basic protein, nf = neurofilaments , PLP = proteolipid protein ; fr = fresh tissue, fi = fixed tissue; ROI = Total ROI analysed , P = no. of patients; MS = Multiple Sclerosis, AD = Alzheimer's Disease , X-ALD = X linked Adrenoleukodystrophy

Table 3.2 Relationship between MRI parameters and ML/AL (R²)

	MD	FA	AD	RD	MTR
ML	0.418 (↑↑)	0.422(↓↓)	0.372(↑)	0.558(↑↑↑)	0.535(↓↓↓)
AL	0.314(↑)	0.401(↓)	0.300(↑)	0.305(↑)	0.443(↓↓)

Abbreviations:

MD = Mean Diffusivity, FA = Fractional Anisotropy, AD = Axial Diffusivity, RD = Radial Diffusivity,

MTR = Magnetization Transfer Ratio ML= Myelin Loss, AL= Axonal Loss

↑ 0.30 < R² < 0.40, ↑↑ 0.41 < R² < 0.45, ↑↑↑ 0.46 < R² < 0.58 (R² value obtained from total random fixed effects model)

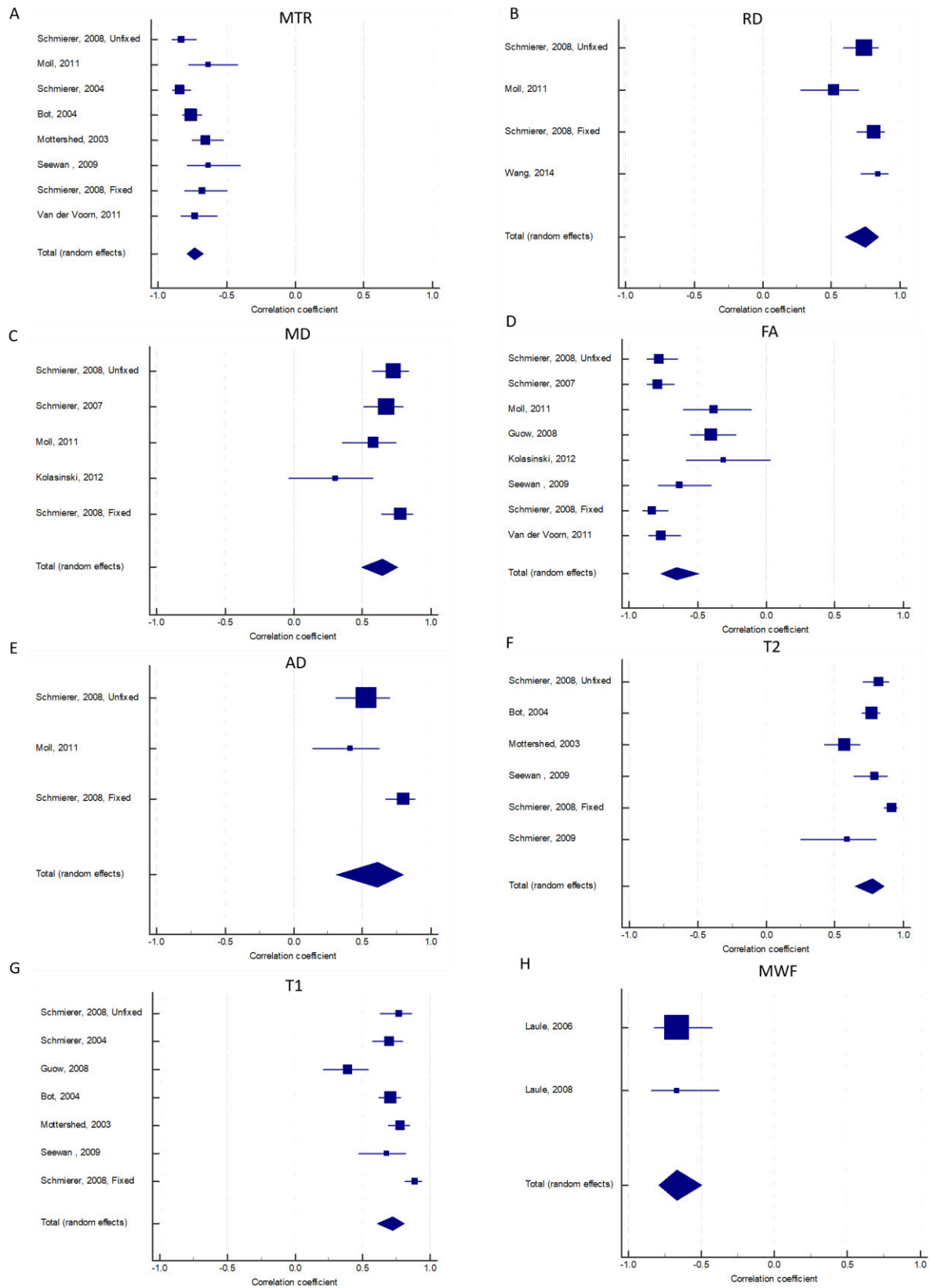


Figure 3-1 Pooled weighted correlation coefficient depicting MRI parameters analysed across various studies against Myelin Loss (ML). (ROI & correlation coefficient) for correlation between myelin loss and either (RD, MTR, AD, FA, MD, T1 relaxation time and T2 relaxation time). Testing for Heterogeneity included 95%CI for I^2 and Q test.

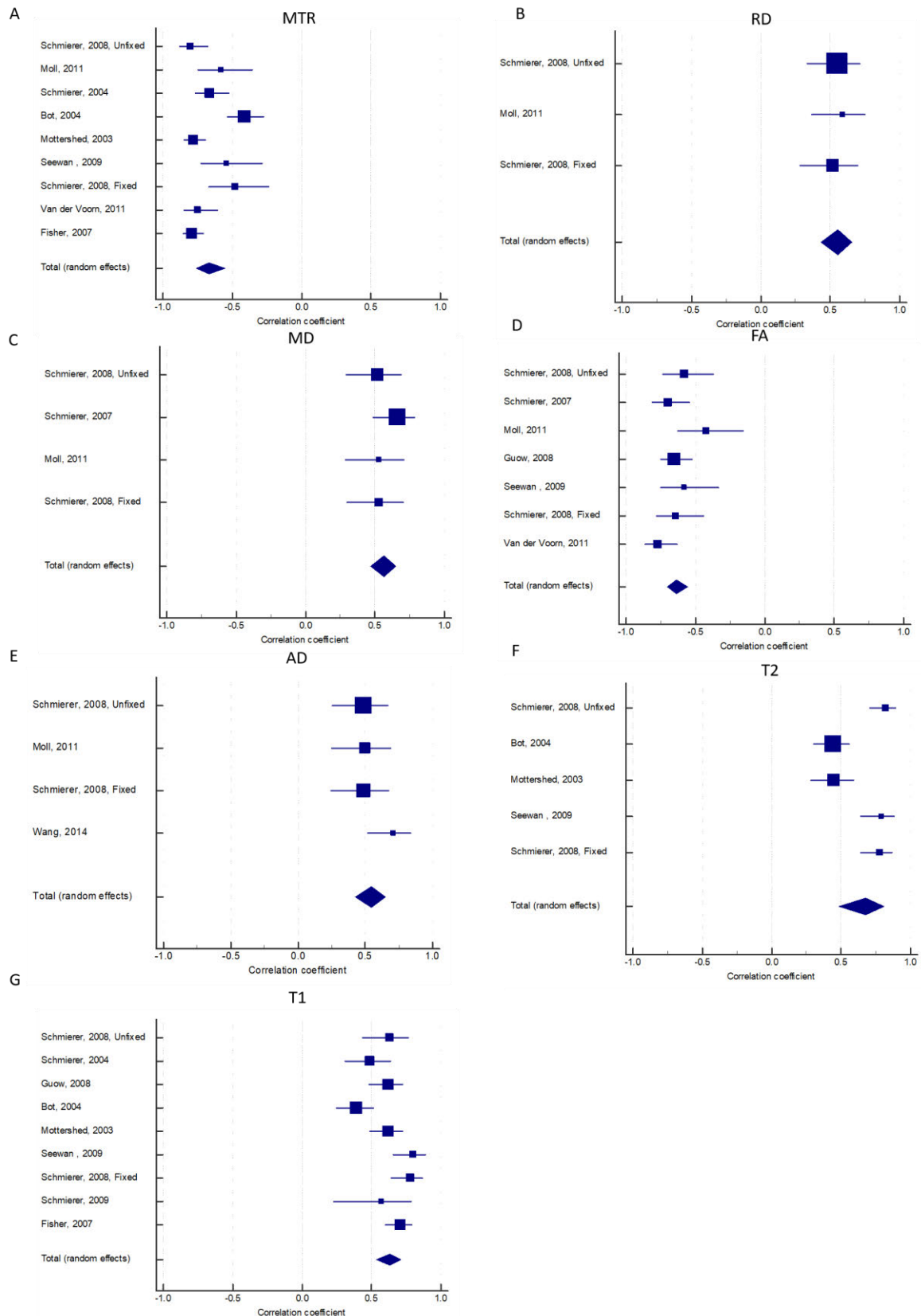


Figure 3-2 Pooled weighted correlation coefficient depicting MRI parameters analysed across various studies against Axonal Loss (AL). (ROI & correlation coefficient) for correlation between myelin loss and either (RD, MTR, AD, FA, MD, T1 relaxation time and T2 relaxation time). Testing for Heterogeneity included 95%CI for I^2 and Q test.

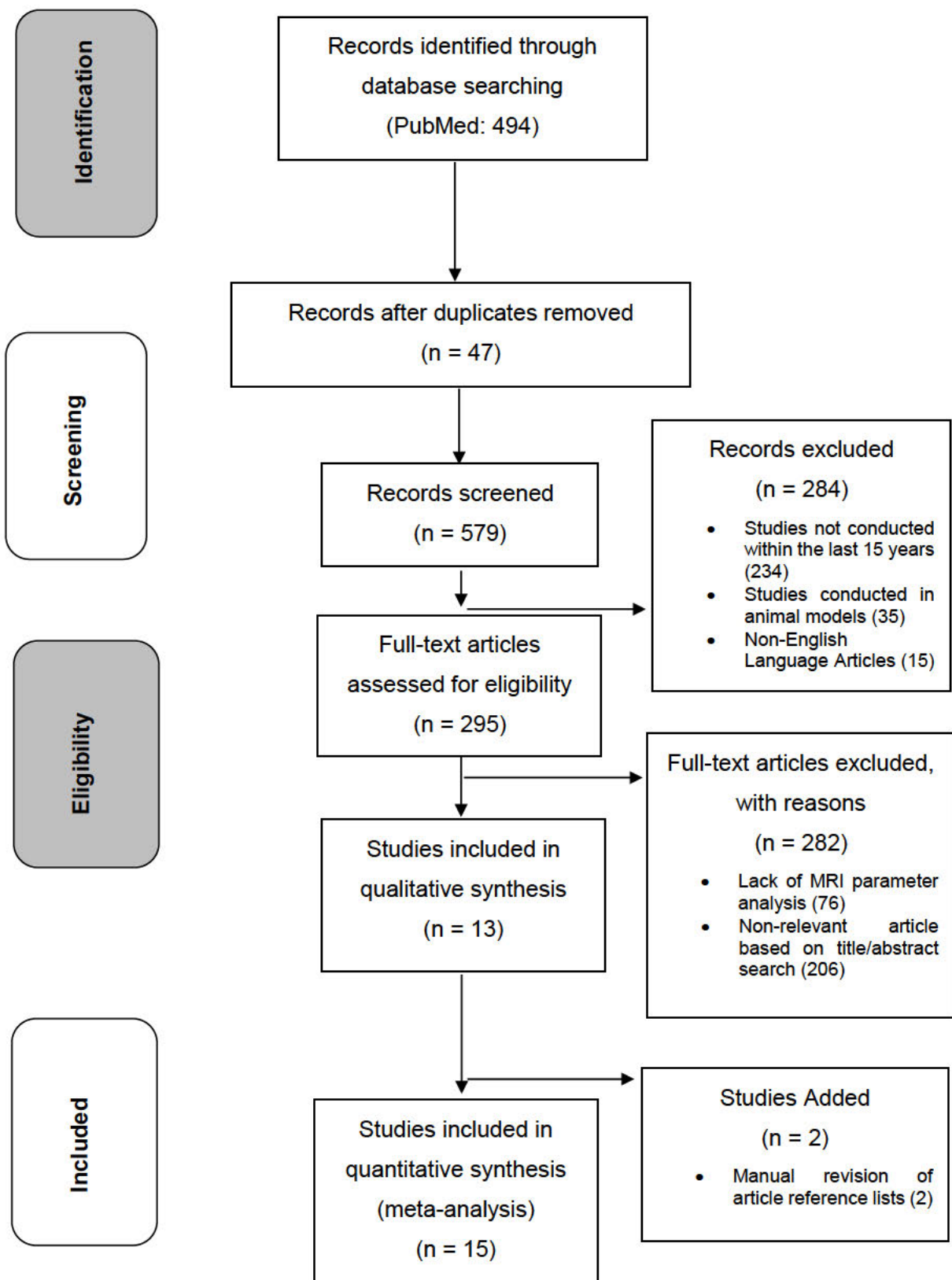


Figure 3-3 (PRISMA) Flow Diagram of Study Selection Protocol

3.5. Discussion

This systematic review was to evaluate and quantify, using available post mortem studies, which MRI sub-parameter is the best predictor of demyelination. Pooled data and statistical analysis were gathered from fifteen studies in order to establish the relationship between histology and neuroimaging. The findings from this analysis revealed that all MRI parameters explored were able to predict both myelin and axonal loss to some extent. The key finding of this study was that the strongest correlation was found between demyelination and two quantitative MRI parameters, MTR and radial diffusivity. It was also found that MTR was overall the best predictor of both myelin and axonal loss in post mortem histological tissue.

MTR has been shown to correlate with histological evidence of demyelination and remyelination [18, 27], and although sensitive to myelin content, the extent of MTR is greatly affected by oedema, inflammation and axonal density thereby, reducing specificity [27]. Nevertheless, previous work in the field has highlighted MTR to be a strong predictor of myelin content in MS brain samples when NAWM lesions were included in the analysis [18]. The correlation between MTR and axonal content has been found to be secondary to the primary association between MTR and myelin content [28, 29]. Work in animal models has shown a strong relationship between demyelination and MTR correlation [30, 31], however when transferred to human studies, histological analysis reveals conflicting results yet again with groups indicating a strong correlation between MTR and demyelination [18, 28, 30, 32] whilst others showed a stronger correlation with axonal density [9, 20, 22]. Our findings agree with Schmierer et al (2008) who found MTR to be the most robust and useful index of myelin content followed by T2/T1 relaxation time and FA, all three indices correlating strongly with myelin content in unfixed tissue and proving advantageous for DTI assessment of MS brains to monitor in vivo changes [2]. MTR remains a promising technique to assess demyelination and is currently one of the few measures of myelin that has been widely applied in clinical trials.

It has been shown through DTI analysis of post mortem spinal cords [33, 34] that radial diffusivity increases with the level of demyelination however, it also similarly increases with axonal loss. When measuring axonal density in isolation, RD was unable to show any correlation however when combined with axonal count simultaneously both features lead

to a specific change in the RD value recorded. As radial diffusivity is strongly related to the myelin content surrounding axons, unsurprisingly axonal loss would lead to an increase in the RD value recorded supporting previously published histopathological animal studies [35, 36]. Whilst demyelination and radial diffusivity seem to be co linked, RD is better at distinguishing regions of milder demyelination compared to normal regions in MS patients [34]. In chronic MS lesions, RD loses specificity for demyelination likely attributed to the advanced tissue damage in late stage MS samples. It should also be noted that one recent study failed to show that relationship between RD and myelin loss and concluded that measure association to not be specific [10]. Overall RD has strong association with demyelination suggesting its use as a potential marker for identification and tissue integrity within early stage MS.

Myelin Water imaging (WMI) is a technique that allows the imaging of myelin associated water and has shown promise in validating chronic WM lesions in post mortem humans [3, 37] . Our correlation of MWF and LFB analysis showed a moderate correlation, indicating that myelin water imaging is a potential and valid MRI marker of myelin content in CNS tissue [24, 37, 38]. MWF is used as a measurement of total myelin content and thus is sensitive to myelin loss. Whilst unable to distinguish between a decrease in myelin due to axonal loss and primary demyelination, its use as a potential MRI marker of demyelination is still up for debate. MWI does however show some promise for clinical use due to its high specificity for myelin, reliability and reproducibility across platforms [27, 37, 39].

The fractional anisotropy value that we received for axonal loss is also of importance clinically. FA has been used in monitoring MS patients clinically and has shown to be increased in many neurological processes within the brain and spinal cord. Ex vivo spinal cord analysis [40] found that demyelination in certain regions of the brain, the main reason for causing an increase in the FA value, with the group concluding that FA is the most robust index derived from DTI analysis and the most specific method for evaluating myelin and axonal pathology. Although the results from this analysis show promise for FA as a potential marker for myelin loss [40], further research is needed in order to help improve or consider its recognition for therapeutic treatment.

MRI parameters are sensitive to many pathological changes in neurological conditions (i.e. myelination, axonal diameter, tissue structure and fibre organisation)[1] and thus

should be interpreted carefully as these pathological changes occur either independently or together in many disease states. There is no one to one relationship between a specific MRI parameter and microstructural change, hence the exact relationship between diffusion MRI and NAWM structure is still unknown. All MRI parameters that we chose to explore in this review, showed some level of correlation with both ML and AL, likely since both pathological changes (ML and AL) are co-linked in human disease. MS being a chronic demyelinating condition leads to loss of myelin and subsequently axons resulting in reduced anisotropy. This result leads to increased diffusion perpendicular to the white matter tract (RD) and as a result and increased overall diffusivity (MD) and decrease in tissue directionality (FA) (See Table 3-2).

Traditionally MS has been thought of as a disease that primarily affects the white matter, with demyelination being a characteristic feature of progressive disease. Post-mortem analysis has been critical in quantifying longstanding disease, however the pathology associated with early demyelinating MS is virtually unknown. Brain biopsy has recently been used to provide pathological evidence of inflammatory demyelination at clinical onset well before radiographic evidence of disseminated MS lesions and myelin loss.

The use of diffusion basis spectrum imaging (DBSI) models together with biopsied brain tissue have been used to report histopathological correlation in living subjects with inflammatory demyelinating MS. The findings from [41] show that both DTI and DBSI measures of RD were significantly increased and consistent with demyelination, with similar findings observed for FA. DBSI results showed more consistency with residual axons whereas DTI measures highlighted confounding effects likely due to an increased water content. DBSI was overall more consistent with histological staining than DTI thus, providing evidence and claiming its use potentially in differentiating coexisting pathologies in MS lesions in vivo.

Our study has also revealed some limitations in the literature which can serve to improve future research in evaluating emerging MRI biomarkers of MS. Although histopathological and MRI combination studies in both animal and humans have demonstrated that there is myelin and axonal combination with in-vivo markers of disease progression, these markers coexist in the human brain, thus separating them has proved challenging and the main limitation of post mortem analysis. The use of highly coherent fibres, such as the optic radiation [42] that run in parallel are more suited to DTI directional analysis as compared to fibres that are multi directional. NAWM fibres located in the brain and spinal

cord vary greatly with direction and length, thus choosing specific fibres for analysis in future post mortem studies would provide a more accurate and quantifiable value for MTR and directional diffusivity measurements respectively. Additionally, fixation presents another hindrance in DTI histological studies. Fixed tissue types decrease water diffusivity whilst anisotropy is preserved [2, 35]. Fixation in human brain samples revealed that RD, AD and MD decreased in unfixed ex vivo brain samples compared to in vivo and dropped further following fixation [8]. This review therefore excluded any studies conducted in animal models and limited inclusion to human studies to allow a more even comparison of MRI parameter results.

This review was aimed at identifying which MRI parameters was the best predictor of demyelination in the central nervous system. We were able to show that MTR and RD were the best predictors of myelin loss in quantitative imaging and histopathological studies.

3.6. Supporting Info

Table 3-1 -Individual Study Characteristics

Figure 3-3 (PRISMA) Flow Diagram of Study Selection Protocol

Figure 3-1 MRI parameters analysed against Myelin Loss (ML)

Figure 3-2 MRI parameters analysed against Axonal Loss (AL)

3.7. Appendices

Appendix 1: Search strategies used when conducting initial literature search

PubMed Search Strategy

	Search Term	Results
1	MRI	556530
2	Demyelination	101860
3	Post Mortem MRI	5857
5	Post-mortem MRI AND Demyelination	410
6	Postmortem MRI AND Demyelination	84

Web of Science Search Strategy

	Search Term	Results
1	MRI	442757
2	Demyelination	25634
3	Post Mortem MRI	2349
5	Post-mortem MRI AND Demyelination	79
6	Postmortem AND MRI and Demyelination	53

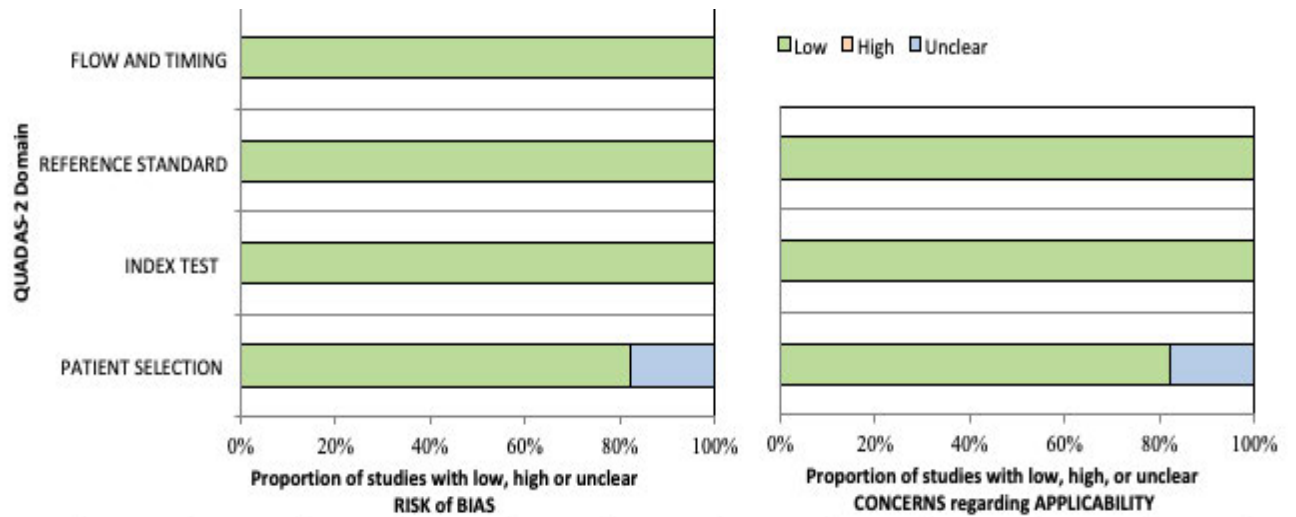
Appendix 2 – PRISMA study Guidelines

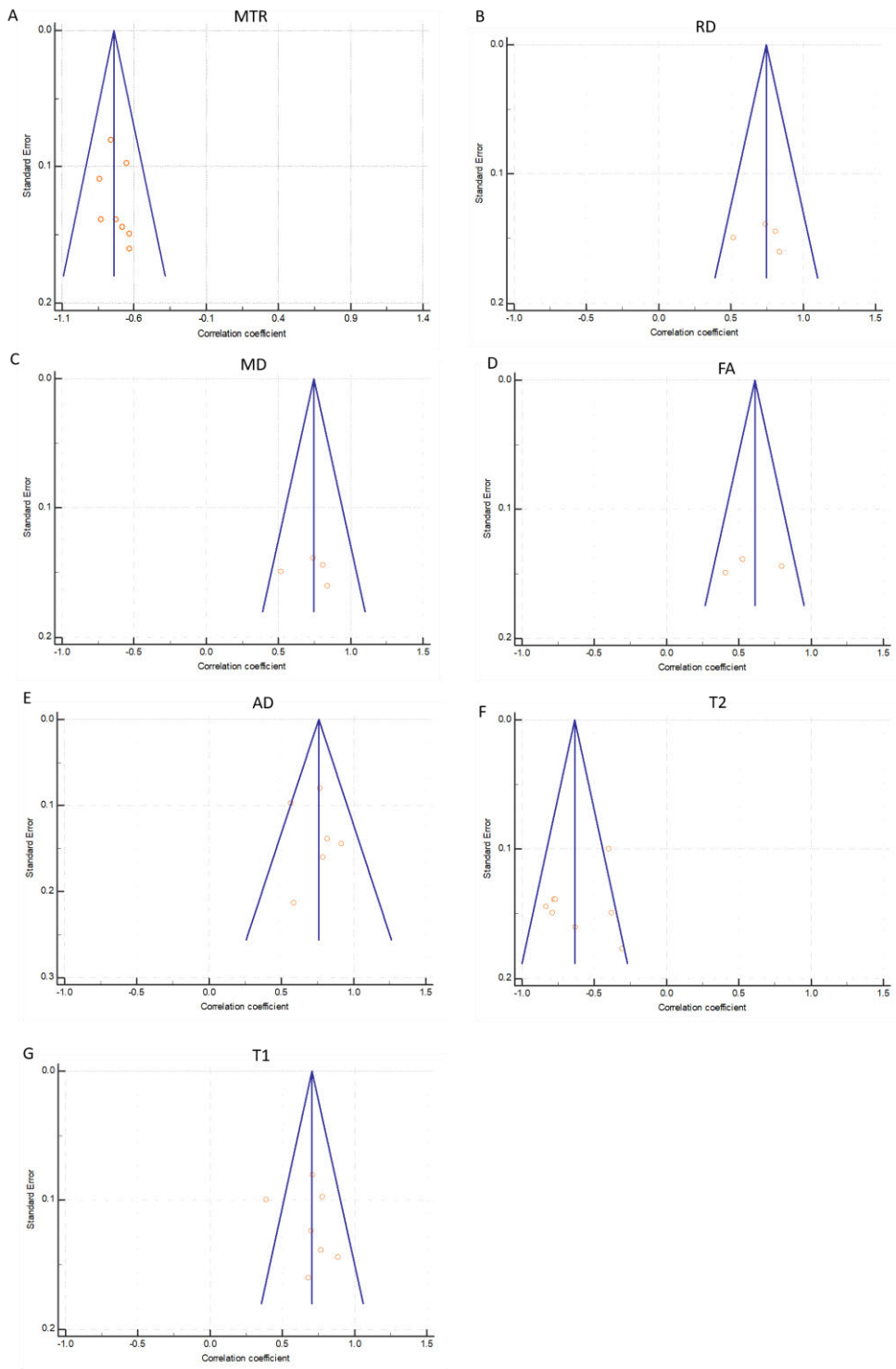
<http://prisma-statement.org/PRISMAStatement/Checklist.aspx>

Appendix 3 – MOOSE study Guidelines

https://www.elsevier.com/ data/promis_misc/ISSM_MOOSE_Checklist.pdf

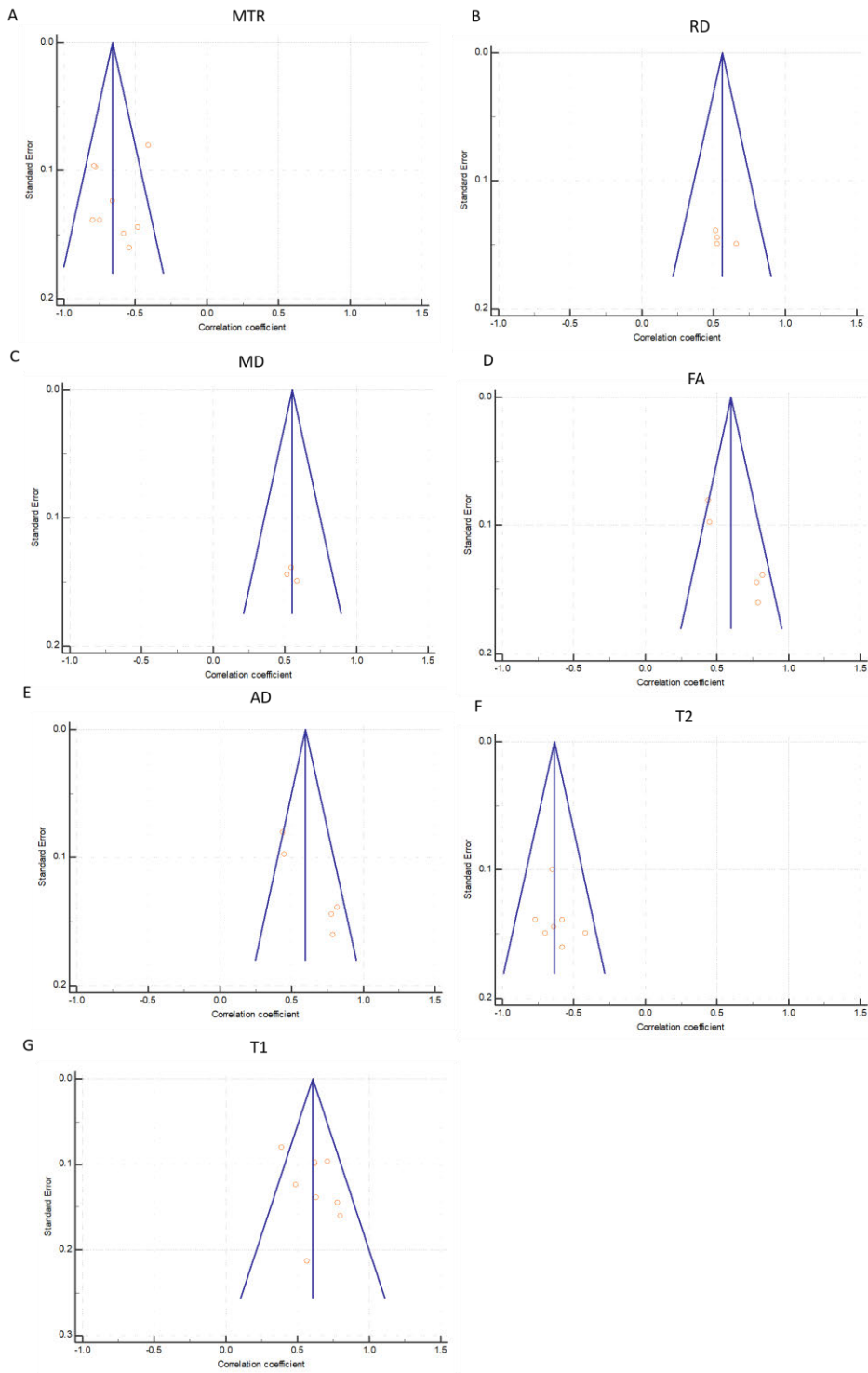
Appendix 4 – QUDAS 2 Methodological Assessment





Appendix -5 Funnel Plots depicting MRI parameters analysed across various studies against (ML)

(Standard error range 0.2-0.0) Statistical analysis included a weighted pooled random effects model (ROI & correlation coefficient) for correlation between myelin loss and either (RD, MTR, AD, FA, MD, T1 relaxation time and T2 relaxation time). Testing for Heterogeneity included 95%CI for I^2 and Q test.



Appendix 6-Funnel Plots depicting MRI parameters analysed across various studies against Axonal Loss (AL).

(Standard error range 0.2-0.0). Statistical analysis included a weighted pooled random effects model (ROI & correlation coefficient) for correlation between myelin loss and either (RD, MTR, AD, FA, MD, T1 relaxation time and T2 relaxation time). Testing for Heterogeneity included 95%CI for I^2 and Q test.

3.8. References

1. Chard, D. and D. Miller, Grey matter pathology in clinically early multiple sclerosis: Evidence from magnetic resonance imaging. *Journal of the Neurological Sciences*, 2009. **282**(1): p. 5-11.
2. Schmierer, K., et al., Quantitative magnetic resonance of postmortem multiple sclerosis brain before and after fixation. *Magnetic resonance in medicine*, 2008. **59**(2): p. 268-277.
3. Laule, C., et al., Myelin water imaging of multiple sclerosis at 7 T: Correlations with histopathology. *NeuroImage*, 2008. **40**(4): p. 1575-1580.
4. de Calignon, A., et al., Propagation of tau pathology in a model of early Alzheimer's disease. *Neuron*, 2012. **73**(4): p. 685-697.
5. Goedert, M., Alzheimer's and Parkinson's diseases: The prion concept in relation to assembled A β , tau, and α -synuclein. 2015. **349**(6248): p. 1255555.
6. Dang, G., et al., Dynamic secondary degeneration in the spinal cord and ventral root after a focal cerebral infarction among hypertensive rats. *Scientific reports*, 2016. **6**: p. 22655-22655.
7. Janve, V.A., et al., The radial diffusivity and magnetization transfer pool size ratio are sensitive markers for demyelination in a rat model of type III multiple sclerosis (MS) lesions. *NeuroImage*, 2013. **74**: p. 298-305.
8. Schmierer, K., et al., Diffusion tensor imaging of post mortem multiple sclerosis brain. *NeuroImage*, 2007. **35**(2): p. 467-477.
9. Van Waesberghe, J.H.T.M., et al., Axonal loss in multiple sclerosis lesions: Magnetic resonance imaging insights into substrates of disability. 1999. **46**(5): p. 747-754.
10. Klawiter, E.C., et al., Increased radial diffusivity in spinal cord lesions in neuromyelitis optica compared with multiple sclerosis. *Multiple sclerosis (Houndmills, Basingstoke, England)*, 2012. **18**(9): p. 1259-1268.
11. Moore, G.R.W., et al., A pathology-MRI study of the short-T2 component in formalin-fixed multiple sclerosis brain. 2000. **55**(10): p. 1506-1510.
12. Kolasinski, J., et al., A combined post-mortem magnetic resonance imaging and quantitative histological study of multiple sclerosis pathology. *Brain : a journal of neurology*, 2012. **135**(Pt 10): p. 2938-2951.

13. Pisanu, A., et al., Systematic review with meta-analysis of studies comparing intraoperative neuromonitoring of recurrent laryngeal nerves versus visualization alone during thyroidectomy. *Journal of Surgical Research*, 2014. **188**(1): p. 152-161.
14. Pisanu, A., et al., Meta-analysis of Prospective Randomized Studies Comparing Single-Incision Laparoscopic Cholecystectomy (SILC) and Conventional Multiport Laparoscopic Cholecystectomy (CMLC). 2012. **16**(9): p. 1790-1801.
15. Abdulla, J., et al., 64-multislice detector computed tomography coronary angiography as potential alternative to conventional coronary angiography: a systematic review and meta-analysis. *European Heart Journal*, 2007. **28**(24): p. 3042-3050.
16. Seewann, A., et al., Diffusely Abnormal White Matter in Chronic Multiple Sclerosis: Imaging and Histopathologic Analysis. *Archives of Neurology*, 2009. **66**(5): p. 601-609.
17. Moll, N.M., et al., Multiple sclerosis normal-appearing white matter: pathology-imaging correlations. *Annals of neurology*, 2011. **70**(5): p. 764-773.
18. Schmierer, K., et al., Magnetization transfer ratio and myelin in postmortem multiple sclerosis brain. 2004. **56**(3): p. 407-415.
19. Bot, J.C.J., et al., Spinal cord abnormalities in recently diagnosed MS patients. Added value of spinal MRI examination, 2004. **62**(2): p. 226-233.
20. Mottershead, J.P., et al., High field MRI correlates of myelincontent and axonal density in multiple sclerosis. 2003. **250**(11): p. 1293-1301.
21. Wang, Y., et al., Differentiation and quantification of inflammation, demyelination and axon injury or loss in multiple sclerosis. *Brain : a journal of neurology*, 2015. **138**(Pt 5): p. 1223-1238.
22. Miller, D.H., et al., High field (9.4 Tesla) magnetic resonance imaging of cortical grey matter lesions in multiple sclerosis. *Brain*, 2010. **133**(3): p. 858-867.
23. Gouw, A., et al., Heterogeneity of white matter hyperintensities in Alzheimer's disease: post-mortem quantitative MRI and neuropathology. 2008. **131**(12): p. 3286-3298.
24. Laule, C., et al., Myelin water imaging in multiple sclerosis: quantitative correlations with histopathology. *Multiple Sclerosis Journal*, 2006. **12**(6): p. 747-753.
25. Fisher, E., et al., Imaging correlates of axonal swelling in chronic multiple sclerosis brains. 2007. **62**(3): p. 219-228.
26. van der Voorn, J.P., et al., Correlating Quantitative MR Imaging with Histopathology in X-Linked Adrenoleukodystrophy. 2011. **32**(3): p. 481-489.
27. Oh, J., et al., Imaging outcome measures of neuroprotection and repair in MS. A consensus statement from NAIMS, 2019: p. 10.1212/WNL.0000000000007099.

28. Barkhof, F., et al., Remyelinated Lesions in Multiple Sclerosis: Magnetic Resonance Image Appearance. *Archives of Neurology*, 2003. **60**(8): p. 1073-1081.
29. Schmierer, K., et al., Stereotactic co-registration of magnetic resonance imaging and histopathology in post-mortem multiple sclerosis brain. 2003. **29**(6): p. 596-601.
30. Deloire-Grassin, M.S.A., et al., In vivo evaluation of remyelination in rat brain by magnetization transfer imaging. *Journal of the Neurological Sciences*, 2000. **178**(1): p. 10-16.
31. Zaaraoui, W., et al., Monitoring demyelination and remyelination by magnetization transfer imaging in the mouse brain at 9.4 T. *Magma (New York, N.Y.)*, 2008. **21**(5): p. 357-362.
32. Dousset, V., et al., Experimental allergic encephalomyelitis and multiple sclerosis: lesion characterization with magnetization transfer imaging. 1992. **182**(2): p. 483-491.
33. Schmierer, K., et al., Quantifying multiple sclerosis pathology in post mortem spinal cord using MRI. *NeuroImage*, 2018. **182**: p. 251-258.
34. Klawiter, E.C., et al., Radial diffusivity predicts demyelination in ex vivo multiple sclerosis spinal cords. *NeuroImage*, 2011. **55**(4): p. 1454-1460.
35. Song, S.-K., et al., Diffusion tensor imaging detects and differentiates axon and myelin degeneration in mouse optic nerve after retinal ischemia. *NeuroImage*, 2003. **20**(3): p. 1714-1722.
36. Song, S.-K., et al., Demyelination increases radial diffusivity in corpus callosum of mouse brain. *NeuroImage*, 2005. **26**(1): p. 132-140.
37. Laule, C., et al., High-resolution myelin water imaging in post-mortem multiple sclerosis spinal cord: A case report. *Multiple Sclerosis Journal*, 2016. **22**(11): p. 1485-1489.
38. Zhang, Y., et al., Pathological correlates of magnetic resonance imaging texture heterogeneity in multiple sclerosis. 2013. **74**(1): p. 91-99.
40. Zollinger, L.V., et al., Using diffusion tensor imaging and immunofluorescent assay to evaluate the pathology of multiple sclerosis. *Journal of magnetic resonance imaging : JMRI*, 2011. **33**(3): p. 557-564.
41. Shirani, A., et al., Histopathological correlation of diffusion basis spectrum imaging metrics of a biopsy-proven inflammatory demyelinating brain lesion: A brief report. *Multiple Sclerosis Journal*, 2018: p. 1352458518786072.
42. You, Y., et al., Demyelination precedes axonal loss in the transneuronal spread of human neurodegenerative disease. *Brain*, 2019. **142**(2): p. 426-442.

4. Normal adjusted RNFL analysis against MRI diffusion parameters within a glaucoma cohort

SHERIFF, S., KLISTORNER, A., GUPTA, VK., GRAHAM, SL., YOU, YUYI. 2019. Retinal Nerve Fibre Layer Analysis against MRI diffusion parameters
(Intended Journal for Review/Publication –IOVS)

4.1. Abstract

Purpose – The main purpose of this study was to investigate the topographic correlation between MRI diffusivity changes in the optic radiation against normalised retinal nerve fibre layer (RNFL) thickness in patients with primary open angle glaucoma (POAG).

Methods – A cross sectional study consisting of 24 POAG patients (10 males and 14 females, age 42 to 77yrs) with superior or inferior visual hemifield loss and corresponding optic disc and retinal nerve fibre layer (RNFL) defects underwent optical coherence tomography (OCT) and Diffusion Tensor Magnetic Resonance Imaging (dtMRI). Presence of RNFL thickness was evaluated via OCT and standardised based on normalised controls for superior and inferior sectors respectively. MRI diffusion parameters, including radial diffusivity (RD), axial diffusivity (AD), mean diffusivity (MD) and fractional anisotropy (FA) were calculated for superior and inferior OR fibres separately and correlated against corresponding sectoral RNFL in each patient. The correlation between MRI parameters and RNFL was analysed using the fixed effects model adjusted for within subject factor.

Results - Combined superior and inferior visual pathway analysis using an adjusted RNFL thickness model showed moderate correlation between RNFL and (RD) ($p = 0.07$) but not (AD) ($p = 0.20$). There was also an association between (MD) and RNFL loss ($p = 0.08$). Mean RNFL thickness in the study population for unaffected sector of the optic disc was ($85.1 \pm 18.22 \mu\text{m}$) as compared to the affected disc sector (62.3 ± 15.845) ($p = 0.0008$).

Conclusion – Analysis of MRI diffusion parameters in the optic radiations projecting to the corresponding visual field in glaucoma showed the greatest correlation between RD

and RNFL, suggesting demyelination as one of the main pathological features in trans synaptic degeneration along the visual pathway.

4.2. Introduction

Glaucoma is a slowly progressing optic neurodegenerative disease that is thought to be the leading cause of irreversible blindness and visual impairment worldwide, with approximately 79.6 million cases reported worldwide [1]. It is characterised through the progressive loss of retinal ganglion cells (RGC's) that result in increased cupping of the optic disc and subsequent thinning of the retinal nerve fibre layer (RNFL), with pathological studies showing that 25-35% of RGC cells are lost before any diagnostic defects appear on standardised visual perimetry (VF) [2]. Primary open angle glaucoma (POAG) is the most common form of the disease [3] with the correlation between increased intraocular pressure and progression of glaucoma already well established, the pathophysiology underlying its spread is still unclear. The current understanding of glaucoma is evolving from a purely ophthalmic condition to a complex neurodegenerative disease involving the entire visual pathway [4]. Trans synaptic or trans neuronal degeneration has been proposed in various neurological conditions including Alzheimer's Disease, Multiple Sclerosis and Parkinson's disease [5, 6], as well as being suggested to occur in glaucoma [4].

The relationship between the glaucomatous retina and the visual pathway in the CNS has been explored in previous studies showing pathological changes especially along the optic radiations (OR) [7-9], however advancements in magnetic resonance imaging (MRI) have shown promise for understanding neurodegeneration in glaucoma in vivo. DTMRI (diffusion tensor magnetic resonance imaging) has emerged as a new method to measure white matter microstructural integrity, revealing other aspects of the neurodegenerative process not previously known [10] as well as being used to examine the retro geniculate pathway in glaucoma patients [11]. Diffusivity indices namely directional measures; radial diffusivity (perpendicular diffusion) and axial diffusivity (parallel diffusion) have been associated with increased levels of demyelination [12, 13] and as such have been used to measure and monitor microstructural changes within neurodegenerative conditions.

The standard method currently available to measure thickness of the RNFL is through advanced imaging techniques such as Optical Coherence Tomography (OCT), first described by Huang(1991) [14] it provides an easy non-invasive method to measure and assess demyelination in the visual system [15]. In addition to being able to quantify RNFL

thickness which may reflect neurodegenerative changes within the brain, thus providing an objective tool to diagnose glaucomatous loss. This trans synaptic degenerative spread of disease from affected to unaffected neurons via synaptic connections [4] may explain the connection between RNFL loss and brain alterations in diseases such as MS and glaucoma.

This study was conducted and draws upon the findings from [16]. Our aim was to investigate the topographic correlation between MRI diffusivity changes in the optic radiations against normalised retinal nerve fibre layer (RNFL) thickness in patients with primary open angle glaucoma (POAG). An analysis was conducted to compare RNFL thickness and correlation against MRI diffusion parameters in order to identify and quantify microstructural changes to provide evidence for trans synaptic degeneration along the visual pathway.

4.3. Methods

4.3.1. Data Collection

MRI glaucomatous changes have previously been investigated in the paper titled *Demyelination precedes axonal loss in the trans neuronal spread of human neurodegenerative disease*. [16]. The aim of this study was to investigate the potential association between MRI and RNFL within the same cohort of patients, to quantify microstructural changes within the superior and inferior optic radiation. Materials and methods for this study have previously been explained and discussed in [16]; A brief overview of the methodological process will be explained in this report with a detailed explanation found in the original paper.

A cross sectional study of primary open angle glaucoma (POAG) patients was conducted to examine RNFL thickness and MRI diffusion parameters. This study was conducted, and study protocols approved by the University of Sydney Human Research and ethics committee (Approval No. 2013/106). Analysis was conducted between The University of Sydney and Macquarie University. Written informed consent was obtained from each participant and the study adhered to the tenets of the declaration of Helsinki.

Subjects were included if they were open angle glaucoma patients with inclusion criteria: (1) primary open angle glaucoma diagnosed by a glaucoma specialist; (2) predominately

superior or inferior hemifield loss, respecting the horizontal meridian; and (3) Corresponding optic disc and retinal nerve fibre (RNFL) defects (Spectralis OCT). Both eyes of each patient were selected and used for analysis.

During the study 48 eyes of 24 subjects were analysed and imaged after inclusion criteria was applied. Twenty-five patients with POAG were enrolled and participated in the current study as well as 27 control subjects with similar age and gender distributions. One patients OCT image quality was not high enough to fulfil the OSCAR-IB criteria for qualitative analysis and was therefore excluded from the study [17].

4.3.2. Spectral Domain Optical Coherence Tomography Imaging

All patients underwent two OCT scans on the same day using the (Spectralis, Heidelberg Engineering, Heidelberg, Germany) OCT including a peripapillary ring scan (SD-OCT RNFL) and a macular radial pattern scan [18, 19]. The macula radial pattern protocol provided six slices in a star-like pattern with the midpoint being the central fovea, and created 12 radial segments around the central fovea, each 4.5 mm long and separated by 30 degrees from each other. All OCT images fulfilled the OSCAR-IB criteria except one [17].

Spectralis OCT software (Version 4.0) allowed for automatic segmentation and separation of the upper and lower RNFL in order to calculate average RNFL thickness. A Heidelberg Spectralis Axonal single exam report OU was generated for each subject and used to calculate the thickness of the RNFL. Peripapillary RNFL thickness values were obtained and divided into four quadrants (Superior, Inferior, Nasal, Temporal). Mean values for both corresponding quadrants in each eye were used to calculate average RNFL thickness for each subject which would be used in the final analysis (Figure 4-1). Superior and inferior OR fibres were generated and fibre based tractography analysis was conducted to reveal diffusivity changes in the corresponding OR projecting fibres to the visual cortex (See Figure 4-1 B)[20].

4.3.3. MRI Data Acquisition

For in depth explanation of MRI data analysis protocol used see [16].

All study participants underwent MRI brain scans on an MR750 3.0 T scanner with an 8-channel head-coil (GE Medical Systems). The VCAT MRI protocol was used

All study participants underwent Glaucoma cohort Axial T1-weighted imaging (inversion recovery fast 3D gradient echo imaging, IRFSPGR) was acquired with the following image parameters: field of view = 240 mm², acquisition matrix (frequency phase) = 342 342, reconstruction matrix: 512 512, phase encoding direction: left to right, echo time = 2.816 ms, inversion time = 450 ms, repetition time = 7.096 ms, pixel bandwidth = 244.141 Hz/pixel, and slice thickness = 0.7 mm. Whole-brain diffusion-weighted images were obtained using an echo planar imaging with 64 gradient directions, field of view = 256 mm, acquisition

matrix = 128 128, reconstruction matrix = 256 256, slice thickness = 2 mm, echo time = 83 ms, repetition time = 8325 ms, bvalue = 1000 s/mm² and two acquisitions without gradient weighting, MRI data acquisition reused with permission from [16].

4.3.4. Statistical Methods

Statistical analysis for this study was completed using (SPSS version 22.0, IBM, USA). Difference between affected and unaffected RNFL was compared by using a paired t test. The correlation was analysed between RNFL and corresponding affected and unaffected MRI parameters in the OR using the fixed effects model. P values less than ($p < 0.05$) were considered as statistically significant

Scatterplots were used to show the relationship between RNFL thickness and MRI diffusion parameters. (See Figure 4-3)

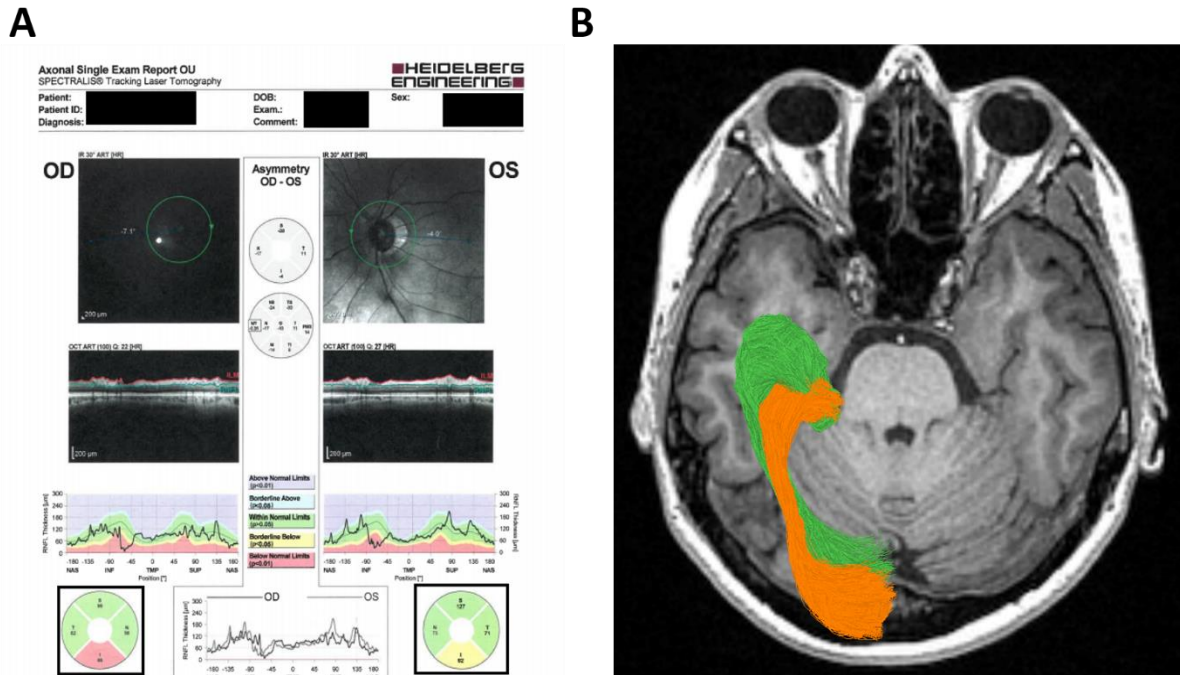


Figure 4-1 Heidelberg Spectralis Axonal single exam report OU printout of a RNFL

(A) Thickness in the normal range is shown in green backgrounds, those that are abnormal at the 5% level are shown in yellow and those that are abnormal at the 1% level are shown in red backgrounds. Average values were taken from corresponding superior and inferior quadrants as seen above and used to calculate RNFL thickness. (B) DTMRI image highlighting that the superior and inferior optic radiations are reconstructed before terminating at the visual cortex (modified with permission [16]). Image for Diagrammatic representation only.

4.4. Results

4.4.1. Patient Characteristics

We recruited twenty-five POAG patients with either superior or inferior visual hemifield loss and corresponding optic disc and retinal nerve fibre layer (RNFL) defects. The mean age for the glaucoma cohort was 64.7 (range 42 to 77yrs), 10 were male (42%) and 14 were female (68%). For the control data used, twenty-seven participants were selected who had an average age of 39.6 with 10 males and 17 females selected.

A comparative analysis was conducted between the 'affected' and 'unaffected' optic radiation in the glaucoma group based on RNFL thickness values that were obtained from

standardisation of normalised controls. The average thickness, anisotropy and diffusivity for each OR are shown in (Figure 4-2) and (Figure 4-3).

4.4.2. Normalised Ratio Calculation

Normalised Affected and Unaffected RNFL measurements were calculated based on control (n=27) patients that were included in the study.

$$G_s = M_n / S_n = 1.02$$

$$G_i = M_n / I_n = 0.979$$

G_s = Normalised Superior, G_i = Normalised Inferior, M_n = Mean Normal value, S_n = Superior Normal OR, I_n = Inferior Normal OR

Each patient's mean superior and inferior RNFL thickness was multiplied by the corresponding ratio (Superior OR to Normalised Superior and Inferior OR to Normalised Inferior) and used in analysis.

Normalised Affected Vs Unaffected RNFL

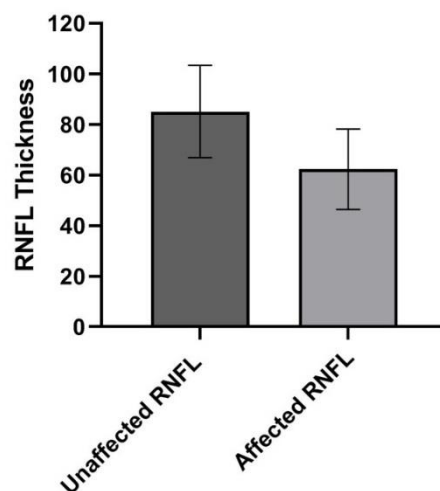


Figure 4-2 Mean +/- SEM for RNFL thickness in the study population

For unaffected OR was (85.1 SD +/- 18.22), compared to Affected OR (62.3 SD +/- 15.845) ($p = 0.0008$).

4.4.3. Mean MRI diffusion parameters

To examine the integrity of white matter throughout the visual pathway, all four DTI parameters, (i.e. FA, MD, RD and AD) were analysed among the glaucoma cohort. Compared with the unaffected OR, All DTI parameters except FA were slightly lower (See Table 4.1). Statistical analysis showed borderline association between RNFL thickness and MRI diffusion parameters in regions that include the visual pathway and neurodegenerative processes. A borderline correlation was detected between adjusted RNFL and radial diffusivity but not axial diffusivity. Paired t tests were used to show statistical significance between examined parameters.

Table 4.1. Average calculated affected and unaffected MRI indices across twenty-four patients.

MRI parameter	Average Unaffected	Average Affected
FA	0.439	0.430
MD	0.862	0.881
RD	0.641	0.659
AD	1.308	1.325

Table 4.2. Correlation between RNFL thickness and DTI variables from twenty-four patients.

Adjusted RNFL vs MRI parameter	p value
FA	p = 0.25
MD*	p = 0.08*
RD*	p = 0.07*
AD	p = 0.20

(* borderline correlation detected)

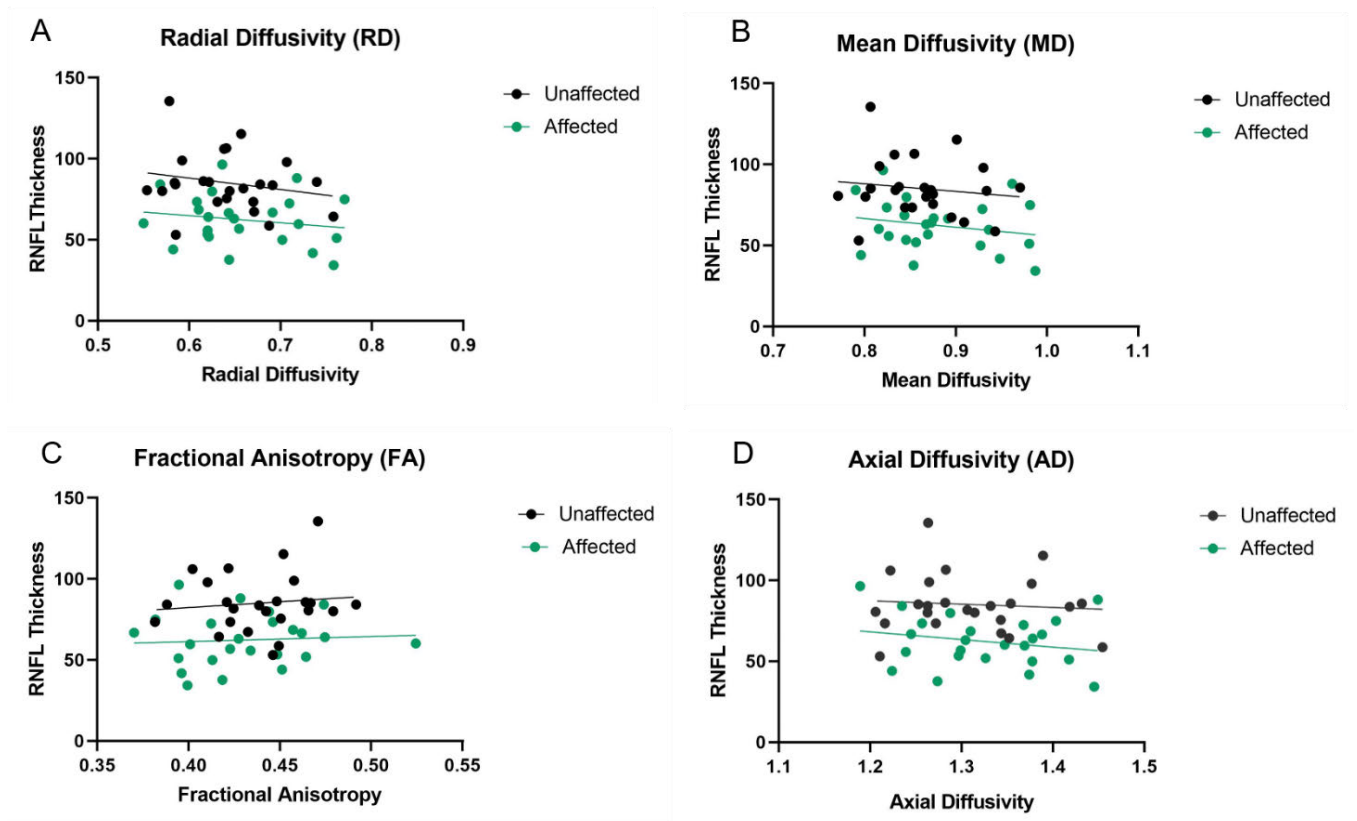


Figure 4-3 Relationship between Retinal nerve fibre layer (RNFL) thickness (μm) and each of the four MRI diffusion parameters between the affected and unaffected optic radiations (OR) in POAG.

The affected OR showed significantly higher axial diffusivity (AD), radial diffusivity (RD), mean diffusivity (MD) measurements as well as lower fractional anisotropy (FA) values when compared to the unaffected OR.

(Graph's modified to show appropriate x axis range for each individual parameter).

4.6. Discussion

Characteristic glaucomatous damage and pathological changes are due to loss of RGC's, since this loss occurs at the RGC level, spread to neighbouring neurons and beyond would require trans synaptic degeneration. The visual pathway provides a unique model by which to study trans synaptic degeneration due to its highly coherent structure of linked neurons that maintain a strong topographic connection throughout the length of the pathway [16]. This allows the examination of pathological damage at one level of the pathway and secondary neurodegeneration to neighbouring neurons. Neuroimaging advancements in recent years has allowed the visual system to be easily accessible and imaged with primary loss of RGC cells easily accessed through functional VF perimetry and through OCT measurement of RNFL thickness and secondary changes similarly examined through fibre tractography and diffusion parameters within the optic radiations and various cortical brain regions[16, 21].

This study was conducted as an extension to the original work published by (You et al 2019), to evaluate and quantify using a cross sectional approach, which MRI sub parameter correlated against a combined superior and inferior pathway analysis using RNFL thickness as a quantitative measure in patients with primary open angle glaucoma (POAG) [16]. Pooled data and statistical analysis were conducted from twenty-four POAG patients as well as twenty-seven controls in order to establish the relationship between RNFL thickness and MRI sub parameters. The findings from this study reveal that the greatest correlation was found between radial diffusivity (RD) but not axial diffusivity (AD) and that the association between non directional parameters was greater for mean diffusivity (MD) than fractional anisotropy (FA).

This study demonstrated a significant loss of RNFL thickness in fibre tracts that corresponded to the optic radiation of the affected or damaged part of the retina, whilst the OR fibres that projected to the unaffected retinal field were spared. This study shows a strong topographic relationship between RGC damage and loss of functionally connected OR fibres providing evidence for structural damage throughout the posterior visual pathway in glaucoma. Another finding that was observed was that despite separating the OR into affected and unaffected sections and considering the considerable amount of RGC damage between the affected and unaffected OR, some DTI parameters showed similar measures in both groups (See Table 4-1). Similar radial diffusivity and

fractional anisotropy changes were observed in both parts of the OR and although there was a similar trend with a higher RD and MD in fibres that were affected than those that were not, the difference was not strong enough to reach statistical significance (See Table 4-2). Axial diffusivity which is a measure of axial flow was the highest recorded parameter and explains the reduction of FA and increase in MD values between the affected and unaffected groups and is in accordance with previous findings [22].

The highest correlation was observed in radial diffusivity which is direction specific perpendicular to axons and suggests that diffusivity is more affected in that direction than along axons in glaucoma [13]. The RD value may provide underlying microstructural changes to structures including demyelination, cell loss, gliosis and microtubule abnormalities as well as suggesting demyelination as one of the main pathological features in trans synaptic degeneration along the visual pathway [23].

The patient cohort included in our study ranged from patients with advanced glaucoma to patients recently diagnosed at baseline, RNFL measurements tend to vary between subjects in cases of advanced glaucoma and are not as sensitive in detecting changes when compared to standardised perimetry. Taliantzis et al (2009) [24] showed that using average RNFL thickness as a measure does not show a strong correlation with VF indices except in patients with progressive structural alterations detected via OCT [24]. Their study concluding that average RNFL does not seem a reliable index for the early detection of glaucoma. Furthermore, we acknowledge that there are some limitations, a relatively small sample size (n=24) may have resulted in a lack of significant difference in MD, and thus may have limited the overall statistical power of DTI measurements within the test group. Axial length measurements were not taken from recruitment subjects during this investigation. The axial length of POAG patients tends to be greater than 26mm which is beyond the normal axial length [25, 26], which may have influenced the correlation between thickness of the RNFL and diffusion parameters.

As a neurodegenerative disease, POAG is a good model to study degenerative changes in the central nervous system. This study has demonstrated that DTI can be a useful tool to quantify microstructural changes corresponding to topographic projections along the visual pathway and thus, be useful as a model of trans synaptic degeneration.

4.8. References

1. Quigley, H.A. and A.T. Broman, The number of people with glaucoma worldwide in 2010 and 2020. 2006. **90**(3): p. 262-267.
2. Kerrigan–Baumrind, L.A., et al., Number of Ganglion Cells in Glaucoma Eyes Compared with Threshold Visual Field Tests in the Same Persons. *Investigative Ophthalmology & Visual Science*, 2000. **41**(3): p. 741-748.
3. Weinreb, R.N. and P.T. Khaw, Primary open-angle glaucoma. *The Lancet*, 2004. **363**(9422): p. 1711-1720.
4. Gupta, N. and Y.H. Yücel, Glaucoma as a neurodegenerative disease. 2007. **18**(2): p. 110-114.
5. de Calignon, A., et al., Propagation of tau pathology in a model of early Alzheimer's disease. *Neuron*, 2012. **73**(4): p. 685-697.
6. Goedert, M., Alzheimer's and Parkinson's diseases: The prion concept in relation to assembled A β , tau, and α -synuclein. 2015. **349**(6248): p. 1255555.
7. Gupta, N., et al., Human glaucoma and neural degeneration in intracranial optic nerve, lateral geniculate nucleus, and visual cortex. 2006. **90**(6): p. 674-678.
8. Yücel, Y.H., et al., Effects of retinal ganglion cell loss on magno-, parvo-, koniocellular pathways in the lateral geniculate nucleus and visual cortex in glaucoma. *Progress in Retinal and Eye Research*, 2003. **22**(4): p. 465-481.
9. Kashiwagi, K.M.O., Toshiyuki MD+; Tsukahara, Shigeo MD*, Association of Magnetic Resonance Imaging of Anterior Optic Pathway with Glaucomatous Visual Field Damage and Optic Disc Cupping. *Journal of Glaucoma*, 2004. **13**(3).
10. Wieshmann, U.C., et al., Diffusion tensor imaging demonstrates deviation of fibres in normal appearing white matter adjacent to a brain tumour. 2000. **68**(4): p. 501-503.
11. Schmidt, M.A., et al., Investigation of lateral geniculate nucleus volume and diffusion tensor imaging in patients with normal tension glaucoma using 7 tesla magnetic resonance imaging. *PloS one*, 2018. **13**(6): p. e0198830-e0198830.
12. Schmierer, K., et al., Quantifying multiple sclerosis pathology in post mortem spinal cord using MRI. *NeuroImage*, 2018. **182**: p. 251-258.
13. Schmierer, K., et al., Quantitative magnetic resonance of postmortem multiple sclerosis brain before and after fixation. *Magnetic resonance in medicine*, 2008. **59**(2): p. 268-277.
14. Huang, D., et al., Optical coherence tomography. *Science (New York, N.Y.)*, 1991. **254**(5035): p. 1178-1181.

15. You, Y., Klistorner, A., Thie, J. and Graham, S.L., Improving reproducibility of VEP recording in rats: electrodes, stimulus source and peak analysis. *Documenta ophthalmologica*, 2011. **123**(2).
16. You, Y., et al., Demyelination precedes axonal loss in the transneuronal spread of human neurodegenerative disease. *Brain*, 2019. **142**(2): p. 426-442.
17. Tewarie, P., et al., The OSCAR-IB Consensus Criteria for Retinal OCT Quality Assessment. *PLOS ONE*, 2012. **7**(4): p. e34823.
18. Graham, E.C., et al., Progressive Loss of Retinal Ganglion Cells and Axons in Nonoptic Neuritis Eyes in Multiple Sclerosis: A Longitudinal Optical Coherence Tomography Study. *Changes in the RGC Layer and RNFL of NON Eyes. Investigative Ophthalmology & Visual Science*, 2016. **57**(4): p. 2311-2317.
19. Shen, T., et al., Differing Structural and Functional Patterns of Optic Nerve Damage in Multiple Sclerosis and Neuromyelitis Optica Spectrum Disorder. *Ophthalmology*, 2019. **126**(3): p. 445-453.
20. Wu, H., J.F. de Boer, and T.C. Chen, Reproducibility of retinal nerve fiber layer thickness measurements using spectral domain optical coherence tomography. *Journal of glaucoma*, 2011. **20**(8): p. 470-476.
21. Kaushik, M., et al., A Topographical Relationship Between Visual Field Defects and Optic Radiation Changes in Glaucoma. *Optic Radiation Changes in Glaucoma. Investigative Ophthalmology & Visual Science*, 2014. **55**(9): p. 5770-5775.
22. Michelson, G., Engelhorn, T., Wärtges, S. et al., DTI parameters of axonal integrity and demyelination of the optic radiation correlate with glaucoma indices. *Arch Clin Exp Ophthalmol*, 2013. **Volume 251**.
23. Klawiter, E.C., et al., Radial diffusivity predicts demyelination in ex vivo multiple sclerosis spinal cords. *NeuroImage*, 2011. **55**(4): p. 1454-1460.
24. Talantzis, S., et al., Comparative studies of RNFL thickness measured by OCT with global index of visual fields in patients with ocular hypertension and early open angle glaucoma. *Clinical ophthalmology (Auckland, N.Z.)*, 2009. **3**: p. 373-379.
25. Yanagisawa, M., et al., Changes in Axial Length and Progression of Visual Field Damage in Glaucoma. *Changes in Axial Length and Progression of Glaucoma. Investigative Ophthalmology & Visual Science*, 2018. **59**(1): p. 407-417.
26. Oliveira, C., et al., Axial length and optic disc size in normal eyes. *The British journal of ophthalmology*, 2007. **91**(1): p. 37-39.

5. Future Directions

5.1. Progression of Trans Synaptic changes in the Glaucoma Cohort

The research undertaken in this Master of Research thesis has so far investigated and described examining the role of trans synaptic degeneration and trans synaptic degenerative changes within glaucoma. Through extensive literature analysis and a clinical study, we were able to show some evidence for MRI parameters (MTR and RD). MTR was overall the best predictor of both demyelination and axonal loss. Of all the diffusivity indices, RD demonstrated the strongest association with demyelination. The association of MRI parameters against myelin loss was overall stronger than the association with axonal loss.

After showing which MRI parameters were the best at measuring demyelination, the next logical step was a clinical study exploring this phenomenon. Glaucoma is a disease with neurological origin as well as involvement of the visual pathway. Hence, was chosen as a model to study trans synaptic degeneration due to its highly coherent and topographic structure. The cross-sectional study that was conducted showed that of all the MRI diffusion parameters that we explored in the meta-analysis previously, the greatest correlation was shown between RD and RNFL. Thus, suggesting demyelination as one of the main pathological features in trans synaptic degeneration along the visual pathway. The cross-sectional study that was conducted was not strong enough to reach a conclusion of causality for trans-synaptic degeneration therefore the next logical step in progression would be to show statistically significant data that correlates microstructural changes in the VP over a period of time within these patients and not solely at baseline measurements.

After collaboration with my research team we chose to follow these glaucoma patients longitudinally over a period of three years, i.e. from baseline to present day (2016 – 2019). This time frame would parallel the progression of glaucoma and would be long enough to show structural changes on MRI imaging.

The Master of Research degree being only 10 months in duration therefore did not allow adequate time in order to carry out this task. So, it was decided that this component would fit in as one of the chapters for my Doctor of Philosophy thesis.

Whilst conducting the literature review and meta-analysis, we began conducting follow up 3-year MRI scans of the original 25 patients that were explored in paper 2. Concurrently, we also conducted VEP analysis and OCT imaging on these same patients in order to extrapolate data from baseline to the end of the study period. Up until this date we have rescanned 9 out of the original 25 patients and look to complete the additional 15 patients within the coming year, therefore allowing analysis to begin as soon as possible.

In conclusion the aim of this research thesis is to provide evidence for trans synaptic degenerative changes within glaucoma and due to the nature of the disease we have shown evidence for trans synaptic changes whilst examining radial diffusivity (RD) as a diagnostic measure of myelin quantification using MRI imaging.

Longitudinally we anticipate some microstructural changes to occur over a period of three years allowing us to come to a final conclusion on MRI parameters and glaucoma progression.

Pages 66-67 of this thesis have been removed as they may contain sensitive/confidential content